A Notch-dependent transcriptional mechanism controls expression of temporal patterning factors in *Drosophila* medulla

Alokananda Ray[1] and Xin Li[1,2]

1. Department of Cell and Developmental Biology, University of Illinois at Urbana-Champaign, Urbana- IL 61801

2. Corresponding author, email: lixin@illinois.edu

Abstract

Temporal patterning is an important mechanism for generating a great diversity of neuron subtypes from a seemingly homogenous progenitor pool in both vertebrates and invertebrates. *Drosophila* neuroblasts have been shown to be temporally patterned by sequentially expressed Temporal Transcription Factors (TTFs). These TTFs are proposed to form a transcriptional cascade based on mutant phenotypes, although direct transcriptional regulation between TTFs has not been verified in most cases. Furthermore, it is not known how the temporal transitions are coupled with generation of the appropriate number of neurons at each stage. We use neuroblasts of the *Drosophila* optic lobe medulla to address these questions, and show that the expression of TTFs Sloppy-paired 1/ 2 (Slp1/2) is regulated at transcriptional level directly by two other TTFs and the cell-cycle dependent Notch signaling through two cis-regulatory elements. We also show that supplying transcriptional active Notch can rescue the delayed transition into the Slp stage in cell cycle arrested neuroblasts. Our findings reveal a novel

20 Notch-pathway dependent mechanism through which the cell cycle progression regulates the
21 timing of a temporal transition within a TTF transcriptional cascade.

22

23 Introduction

24 Generation of a great diversity of neurons from a small pool of neural progenitors is critical for
25 constructing functional nervous systems. This is achieved in part by integration of temporal
26 patterning and spatial patterning of neural progenitors [reviewed in [1-4]]. Temporal patterning of
27 neural progenitors refers to the generation of differently fated progeny in a birth-order
28 dependent manner, and this is observed in both invertebrates and vertebrates [reviewed in [5-7]
29]. The central nervous system in *Drosophila melanogaster* has been an excellent model to study
30 temporal patterning. Neural progenitors called neuroblasts (NBs) have been shown to
31 sequentially express series of temporal transcription factors (TTFs), which are each required to
32 specify subsets of neuron fates [reviewed in [8,9]]. For example, neuroblasts in the embryonic
33 ventral nerve cord (vnc) are temporally patterned by a TTF cascade Hunchback (Hb), Kruppel
34 (Kr), Nubbin/Pdm2 (Pdm), Castor (Cas) and Grainy head (Grh) [10-13], while *Drosophila* optic lobe
35 medulla neuroblasts utilize a different TTF cascade composed of Homothorax (Hth), SoxNeuro
36 (SoxN), Doublesex-Mab related 99B (Dmrt99B), Odd paired (Opa), Eyeless (Ey), Earmuff (Erm),
37 Homeobrain (Hbn), Sloppy-paired (Slp1,Slp2), Scarecrow (Scro), Dichaete (D), BarH1/2, Tailless
38 (Tll), and Glial cell missing (Gcm)[14-19]. In these TTF cascades, cross-regulations were identified
39 among TTF genes based on loss and gain of function phenotypes, and they were proposed to
40 form a transcriptional cascade [11-13, 14-19,20] that can in theory self-propagate [21]. However, with a

41 few exceptions [22], the cis-regulatory elements of these TTF genes haven't been characterized,
42 and thus it is not known whether these cross-regulations are indeed direct transcriptional
43 regulations. Moreover, in the embryonic TTF cascade, although mis-expression of one TTF is
44 sufficient to activate the next TTF and repress the "next plus one" TTF, loss of one TTF often
45 does not block temporal progression, but only causes the corresponding fates to be skipped [11].
46 In the medulla TTF cascade, one TTF is required but not sufficient to promote the TTF cascade
47 progression [19]. These studies suggest that additional mechanisms in addition to cross-
48 regulations among TTFs might function to regulate TTF progression.
49
50 As the neural progenitors go through the TTF cascade, they need to generate a certain number
51 of postmitotic progeny as each temporal stage. Therefore, it has been questioned whether cell
52 cycle progression is required for the TTF cascade progression. In the embryonic VNC TTF
53 cascade, cytokinesis is required for the first transition (Hb to Kr) by promoting the nuclear
54 export of seven-up (*svp)* mRNA encoding a switching factor, but all later temporal transitions
55 progress normally in G2-arrested neuroblasts [11,23,24]. In larval VNC NBs, timely transition from
56 the Imp /Castor/Chinmo to Syncrip/Broad stage also requires cell cycle progression [25]. These
57 results suggest that the requirement of cell-cycle progression varies depending on the specific
58 temporal transition. In vertebrate cortical progenitors, the temporal transition from generating
59 deep layer neurons to generating upper layer neurons is not affected by blocking cell cycle
60 progression when constitutively active Notch signaling is provided [26]. However, it is still
61 possible that Notch signaling might be promoting the temporal transition in the absence of cell
62 cycle progression.

63

64 Notch signaling plays pleiotropic roles in neurogenesis and neural development in both
65 vertebrates and invertebrates [reviewed in [27]]. Upon binding to a ligand from a neighboring
66 cell, the Notch receptor is cleaved to release the Notch intracellular domain (NICD), which then
67 enters the nucleus and associates with the DNA-binding protein CSL (CBF1/RBPjκ/Su(H)/Lag-1).
68 The NICD-CSL then recruits transcriptional coactivator Mastermind (MAM) to activate
69 transcription of Notch target genes, mainly the bHLH transcriptional repressors of the HES
70 (hairy and enhancer of split) /HEY families [reviewed in [28-30]]. Drosophila NBs divide
71 asymmetrically multiple times and at each division generate a self-renewed neuroblast and a
72 more differentiated progeny, that is either an intermediate progenitor [Ganglion Mother Cell
73 (GMC) for type I NBs, or Intermediate Neural Progenitor (INP) for type II NBs], or a postmitotic
74 progeny (type 0 NBs) [reviewed in [31]]. During the asymmetric division of Drosophila
75 neuroblasts, Numb, a negative regulator of Notch signaling, is asymmetrically localized to the
76 intermediate progenitor, resulting in unidirectional Delta-Notch signaling from the intermediate
77 progenitor to the neuroblast [32-35]. Ectopic activation of Notch signaling in the progeny causes
78 them to revert back into neuroblasts and over-proliferate, while inhibition of Notch signaling in
79 type II NBs eliminated the whole lineage [36-39]. In contrast, in most type I NB lineages, loss of N
80 signaling does not affect neuroblast maintenance, and it was shown that E(spl) complex
81 proteins and Deadpan act redundantly to maintain the un-differentiated state (stemness) of
82 neuroblasts by repressing differentiation genes [39-41]. Notch signaling is also involved in
83 controlling the daughter cell proliferation modes specifically the type I to type 0 switch in
84 embryonic VNC NBs [42,43]. Work in vertebrate central nervous system suggest that during the

85 asymmetric division of neural progenitors, the more differentiated progeny expresses Delta and
86 activates Notch signaling in the sister cell to maintain the neural progenitor fate [reviewed in
87 [27]]. In addition, Notch signaling show cell cycle dependent activation and the expression of
88 Notch target Hes genes oscillates during the cell cycle in neural progenitors [reviewed in [44]].
89 Although Notch signaling has been shown to play many important roles in neural lineage
90 development, whether Notch signaling also has a role in temporal transitions between TTFs has
91 not been investigated.
92 Here, we use *Drosophila* medulla neuroblasts to address these questions. In the larval optic
93 lobe, a neurogenesis wave spreads in a medial to lateral direction to sequentially convert
94 neuroepithelial cells into neuroblasts. As a result, medulla neuroblasts of different ages are
95 orderly aligned on the lateral to medial spatial axis with the youngest on the lateral side (Fig.
96 1A). Medulla neuroblasts divide asymmetrically multiple times to self-renew and to generate a
97 series of GMCs and at the same time they transit through the TTF sequence (Fig. 1A). Among
98 the TTFs, Slp1 and Slp2 are two homologous fork-head family transcription factors expressed in
99 the same temporal pattern in medulla neuroblasts (Fig. 1B-B'''). In this work, we identified two
100 cis-regulatory enhancer elements that regulate the temporal expression pattern of Slp1/2, and
101 showed that the previous TTF Ey, another TTF Scro, and the Notch signaling pathway directly
102 regulate the transcription of *slp* through these two enhancers. Slp1/2 expression is delayed
103 when N signaling is lost or when cell cycle progression is blocked which also causes loss of N
104 signaling. Furthermore, we show that supplying transcriptionally active Notch can rescue the
105 timely Ey to Slp transition in cell-cycle arrested neuroblasts. Thus, our work demonstrates that

106 cell-cycle dependent Notch signaling cooperates with TTFs to promote the progression of the
107 TTF transcriptional cascade.
108

109 Results

110 **Expression of Slp1 and Slp2 in medulla neuroblasts is regulated at the level of transcription by**
111 **coordinated function of at least two enhancers.**

112 The observed distribution of temporal patterning transcription factors may be regulated at
113 either the transcriptional or post-transcriptional level, and the protein expression pattern is not
114 necessarily the same as that of the mRNA transcripts. A case in point is the expression pattern
115 of the SoxN protein recently reported to function alongside Dmrt99B and Hth to specify
116 identities of early-born neurons in the medulla; while mRNA transcripts of soxN gene are widely
117 distributed in neuroblasts, SoxN protein is only expressed in the youngest neuroblasts,
118 suggesting that post-transcriptional mechanisms are at work to confine the actual domain of
119 SoxN protein expression[17]. To examine whether the expression of Slp1/2 in medulla
120 neuroblasts is regulated at transcription, we observed the distributions of *slp1* and *slp2* mRNA
121 transcripts by fluorescence *in situ*-hybridization (Fig. 1C-C'''). The observed patterns of *slp1* and
122 *slp2* mRNA expression closely parallel the expression of Slp1 and Slp2 proteins (Fig. 1B-B'''), and
123 are also corroborated by scRNA-seq data[17], indicating that the expression of *slp1* and *slp2* is
124 directly regulated at transcription.

125 We then sought to identify transcriptional enhancers that enable expression of the *slp* genes in
126 the characteristic pattern observed in medulla neuroblasts. From our examination of expression

127 patterns of GFP in third instar larval brains driven by Gal4 lines under the regulation of putative
128 enhancer elements [45-47] (available from the Janelia FlyLight image database
129 https://flweb.janelia.org/cgi-bin/flew.cgi), we identified the GMR35H02 Gal4 line as containing a
130 candidate enhancer driving Slp1/2 expression in medulla neuroblasts. We then verified the
131 expression of UAS-GFP driven by GMR35H02-Gal4 and found that indeed the GFP expression in
132 medulla neuroblasts was initiated at the same time as endogenous Slp1 and Slp2
133 (Supplementary Fig. S1A-B'). Subsequently, we cloned the 3.75 kbp element corresponding to
134 the GMR35H02 Gal4 regulatory sequence upstream of a EGFP reporter gene with a basal hsp70
135 promoter in the vector pJR12[48] and constructed transgenic lines. In these lines GFP was
136 expressed in the same pattern as the GMR35H02Gal4 driving UASGFP. Through successive
137 iterations of enhancer-bashing experiments whereby we cloned progressively smaller segments
138 of the initial 3.75 kbp element (See Supplementary Table 1 for primer sequences used) in the
139 above-described vector and observed GFP reporter expression in transgenic flies, we identified
140 a 220 bp fragment within the larger GMR35H02 regulatory DNA which preserved the expression
141 pattern of the GFP reporter (Fig. 1E-E''') as that of UAS-GFP driven by the GMR35H02 -Gal4.
142 This we reasoned is a minimal enhancer driving expression of Slp genes in medulla neuroblasts.

143 Deletion of this element by CRISPR-Cas9 however failed to completely eliminate the expression
144 of Slp1 and Slp2 in neuroblasts (Supplementary Fig. S1C-C'''), though it noticeably reduced the
145 expression domain of Slp1 (Supplementary Fig. S1E). Given the likelihood of developmentally
146 regulated gene expression being controlled by multiple enhancers [49,50] and the importance of
147 enhancer redundancy to achieving robust developmental outcomes [49,51,52], this hinted that
148 other enhancers may act redundantly to regulate Slp1/2 expression in medulla neuroblasts. We

149 identified other potential enhancers of Slp1/2 expression from the REDfly database[53,54] and
150 tested their roles in driving Slp1/2 expression in the context of medulla neuroblasts. We
151 screened available transgenic lines expressing GFP or lacZ reporters driven by putative
152 enhancer elements (kind gifts from Dr. Miki Fujioka and Dr. James B. Jaynes) and cloned other
153 candidate regulatory segments in the pJR12 GFP-reporter vector to compare GFP transgene
154 expression to endogenous Slp1/2 expression. Through this screen we identified a second
155 regulatory segment corresponding to the REDfly enhancer d5778 (Fig. 1D) that can drive GFP
156 expression in medulla neuroblasts within the endogenous Slp1/2 expression domain.
157 Subsequently we found that an 850 bp segment within the d5778 enhancer is sufficient to
158 initiate GFP expression in this pattern (Fig. 1F-F'''). Reporter expression driven by this second
159 enhancer (henceforth referred to as d5778 850bp enhancer) is initiated at a slightly later time
160 compared to the first identified enhancer, in older Slp expressing neuroblasts and also in glial
161 cells at the junction of the medulla and the central brain. Our analysis of the REDfly enhancers
162 that supposedly regulate expression of Slp1/2 also revealed that the earlier identified 220 bp
163 enhancer segment is contained within another REDfly enhancer named u8772 (Fig. 1D). Thus,
164 we refer to the first identified enhancer henceforth as u8772 220bp. As in case of the u8772
165 220bp enhancer deletion, sole deletion of d5778 enhancer by CRISPR-Cas9 again did not abolish
166 Slp1/2 expression(Supplementary Fig. S1D-D'''), suggesting that these enhancers function
167 redundantly and may make additive contributions to attaining the observed levels of Slp1 and
168 Slp2 expression.

169 Bioinformatic analyses of the sequences of our identified enhancers (see Methods) identified
170 binding sites for the previous TTF Ey, the CSL transcription factor Su(H), Slp1 itself, and a Nk2-

171 class homeodomain transcription factor ventral nervous system defective (vnd) (Supplementary
172 Table 2). The previous TTF Ey has been shown to be required but not sufficient for activating Slp
173 genes' expression in medulla neuroblasts, but it was not known whether this regulation is
174 direct. Vnd is not expressed in medulla neuroblasts according to our single-cell RNA-sequencing
175 data[17], but a related homologous NK-2 homeobox transcription factor Scarecrow[55] (Scro) is
176 expressed around the same time as Slp, and loss of Scro leads to significantly reduced Slp
177 expression level[17]. The CSL transcription factor Su(H) is the *Drosophila* homolog of RBP-J[56,57],
178 and the key DNA-binding component of the active Notch transcriptional complex. The Notch
179 signaling pathway plays an overarching role as a master regulator of development and
180 differentiation in neuroblasts, but it hasn't been shown to regulate the expression of temporal
181 patterning genes in neural progenitors. Therefore, we next tested whether Slp1/2 expression is
182 regulated by Notch signaling.

183 **<u>The Notch pathway regulates Slp1 and Slp2 expression in medulla neuroblasts</u>**

184 We observed expression of Slp1 and Slp2 in RNAi knockdown clones of key Notch pathway
185 components induced by *ayGal4* (*actin>FRT-y$^+$-STOP-FRT-Gal4*, in which *actin* promoter drives
186 Gal4 expression only after a STOP cassette is excised by the action of heat shock activated
187 Flippase[58]). Since Slp1 and Slp2 are two homologous genes located in proximity [59] and
188 expressed in patterns very similar to one another with the timing of Slp1 expression slightly
189 preceding that of Slp2 expression (Fig. 1B-B'''), in all subsequent figures we have shown data for
190 Slp2 only with the assumption that Slp1 expression reflects the same pattern. On inducing RNAi
191 knockdowns of the critical Notch pathway components Notch and Su(H) – which are part of the
192 tripartite core of the active Notch transcriptional complex [60], it is seen that Slp2 expression is

193 delayed within the RNAi knockdown clones marked by GFP expression (Fig. 2A-A’’’, B-B’’’
194 respectively) compared to wild type neuroblasts of the same age (i.e., in the same vertical
195 ‘stripe’). A similar effect is seen when dominant negative variant of the third core component of
196 the Notch transcriptional complex mastermind (mam) is expressed under the control ayGal4
197 (Fig. 2C-C’’’). These data suggest that timing of Slp1/2 expression in medulla neuroblasts is
198 regulated by the Notch pathway.

199 To identify the cognate ligand of Notch that functions in activating the Notch signaling in
200 medulla neuroblasts, we examined expression of known Notch ligands- Delta [61], Serrate[62,63] and
201 Weary[64] in medulla neuroblasts (data not shown). Of these only UAS-GFP driven by Delta-Gal4
202 was seen to be expressed in medulla neuroblasts and in their progeny GMCs. We then
203 examined whether loss of Dl recapitulates the effects we observe on Slp1/2 expression with
204 loss of function of core Notch transcription complex components, if indeed Dl is required for
205 activating Notch signaling in these cells. RNAi knockdown of Dl resulted in a similar delay in
206 initiating Slp2 expression as with loss of function of other key actors in the Notch pathway (Fig.
207 2D-D’’’) confirming this expectation.

208 **<u>Notch pathway and Ey regulate the activity of *slp* enhancers.</u>**

209 Since Su(H) and Ey are required for Slp expression, we next tested whether these regulations
210 are mediated through the identified enhancers. We tested whether knockdown of each factor
211 would affect GFP reporter expression driven by these enhancers. We reasoned that if any of the
212 factors we had identified binding sites for bound to the enhancers and enabled them to initiate
213 Slp1/2 transcription, GFP reporter expression driven by these enhancers would be lost in loss of

214 function clones of these transcription factors. We induced RNAi knockdown clones for Ey and
215 Su(H) using ayGal4 in transgenic flies expressing wild type GFP reporters driven by these two
216 enhancers and compared the expression of GFP in wild type neuroblasts and in neuroblasts
217 where each of these TFs had been individually knocked down.

218 For both enhancers, GFP reporter expression was lost in *eyRNAi* clones (Fig 3A-B') confirming an
219 earlier observation that Ey was required for initiating Slp1/2 expression. It also strengthened
220 the evidence that these two were indeed bona-fide enhancers activating Slp1/2 expression.
221 Similarly, GFP reporter expression was lost or delayed in s*u(H) RNAi* clones for both enhancers
222 (Fig 3C-D'), confirming that Su(H)/N pathway regulates Slp1/2 expression through these two
223 enhancers. Since Slp binding sites were also identified in the *slp* enhancers, we next tested the
224 effect of loss of Slp1/2 function on the expression of our GFP reporters. To this end we induced
225 *slp1/2* loss of function (LOF) mutant clones in flies carrying the *GFP reporter and UbiRFP*
226 *FRT40A*. In Fig. 3E-F' *slp* LOF clones are visible as dark regions devoid of RFP whereas wild type
227 neuroblasts are marked by RFP expression from the Ubiquitin promoter. Reporter expression
228 driven by both enhancers within *slp* LOF neuroblasts is normal as in wild type neuroblasts.
229 Though this suggests that Slp1/2 are not required to initiate their own expression, it does not
230 preclude a possible role of Slp1/2 in sustaining their own expression in older Slp1/2 stage
231 neuroblasts or progeny, but the perdurance of the GFP reporter prevents us from testing this
232 possible role. In summary, our genetic experiments confirmed that identified enhancers of
233 *slp1/2* respond to activation by Ey and Su(H).

234 **Mutations of potential binding sites for Ey, Su(H) and Scro in *slp1/2* enhancers impair**
235 **expression of the reporters**

236 To further test whether the regulators we identified indeed regulate Slp1/2 expression directly
237 through binding to the enhancers, we set out to mutate all possible binding sites for each of the
238 regulators- Ey, Su(H), Scro and Slp1, on each enhancer. We identified all potential matches to
239 consensus binding motifs for these factors using the DNA Pattern Recognition Tool within the
240 Sequence Manipulation Suite[65]. Custom-designed gene blocks containing the mutated
241 enhancer sequences were cloned upstream of the GFP reporter in pJR12 vector as before, and
242 transgenic flies expressing these reporter constructs were then made (Supplementary Table1).
243 We next compared the expression patterns and intensities of GFP reporters with mutated TF
244 binding sites against GFP reporter expression driven by the 'wild type' version of that same
245 enhancer (Fig. 4A-A''', Fig. 5A-A'''). To compare GFP reporter intensities between wild type and
246 mutated variants of an enhancer, identical microscope illumination and imaging settings were
247 used for all variants of the same enhancer.

248 Mutation of all potential Ey binding sites nearly eliminated GFP expression for both enhancers
249 (Fig. 4B-B''', F and Fig. 5C-C''',F), as did the mutation of all possible Su(H) binding sites (Fig. 4C-
250 C''', F and Fig. 5D-D''',F). For the d5778 850 bp enhancer, the expression of GFP in glial cells is
251 still present and likely intensified when Su(H) binding sites are mutated. Since it is impossible to
252 avoid contributions to the GFP signal intensity from surface-glial cells in neuroblast stacks we
253 have quantified, the GFP signal intensity reflected in our measurements for the d5778 Su(H)
254 site mutant reporter seems high and also very variable (Fig. 4F). However, GFP expression from
255 the d5778 Su(H) site mutated reporter in neuroblasts alone is dramatically reduced compared
256 to the wild type. Mutation of scro sites in the u8772 220bp enhancer also led to a loss of GFP
257 expression (Fig. 4D-D''',F), whereas GFP expression was considerably weakened in the d5778

258 850bp scro site mutant enhancer (Fig. 5B-B’’’,F). In contrast, mutation of Slp1 binding sites did
259 not significantly affect the reporter expression (Fig. 4E-E’’’, F, and Fig. 5E-E’’’). In summary, our
260 results provided strong evidence that Ey, Su(H) and Scro directly regulate Slp1/2 expression
261 through binding to its two enhancers.

262 **DamID-sequencing confirms binding of Ey and Su(H) to identified enhancers of Slp1/2.**

263 DamID-sequencing can be used to profile genome-wide binding patterns for transcription
264 factors and chromatin proteins [66,67]. We used a *SoxN*Gal4 that is expressed in all medulla
265 neuroblasts[17] to drive the expression of UAS-DamSu(H) or UAS-DamEy fusion proteins, and
266 inferred the genome-wide binding patterns of Ey and Su(H) through DamID-sequencing. For
267 each transcription factor two biological replicates were sequenced. Reproducible peaks of Ey
268 and Su(H) binding were observed in both replicates in the genomic region corresponding to the
269 identified enhancers of Slp1/2 transcription (Fig. 6A). Additionally, we also observed peaks of Ey
270 and Su(H) binding in the genomic region of *scro* gene (Supplementary Fig. S2A). It has been
271 reported that Scro expression is initiated in medulla neuroblasts at about the same time as
272 Slp1/2. This raises the possibility that Scro expression may also be initiated by either Ey, Su(H)
273 or both. In another temporal gene *homeobrain* (*hbn*) that is turned on in the Ey stage [16,18], Ey
274 and Su(H) binding peaks were also observed (Supplementary Fig. S2B). Genome-wide about
275 62.78% of all Su(H) bound genes and 60.3% of all Ey bound genes were bound by both Ey and
276 Su(H) (Fig. 6B). Enriched GO terms for these co-bound genes include: neuroblast fate
277 determination, cell division, asymmetric cell division, apical cell polarity, Notch signaling
278 pathway and axon guidance (Fig 6C-H). Taken together these data support evidence from our

279 genetics studies and together they suggest that Ey and Su(H)/N pathway activate Slp1/2
280 transcription by direct binding to Slp1/2 enhancers.

281 **Notch signaling is dependent on cell-cycle progression.**

282 Although it has been well-established that GMCs generated by the asymmetric division of
283 neuroblasts signal to their sister neuroblasts to provide the Notch signaling[32,33], it hasn't been
284 demonstrated whether Notch signaling is lost in cell-cycle arrested medulla neuroblasts since
285 they fail to generate GMCs. We used a regional Gal4, *vsxGal4* that is expressed in the center
286 domain of the medulla crescent starting in the neuroepithelium[68], to drive UAS-DCR2 and a
287 RNAi line against Proliferating Cell Nuclear Antigen (PCNA),which is essential for DNA
288 replication and S phase progression[69]. Blocking cell cycle progression caused premature
289 transformation of neuroepithelial cells to neuroblasts, as has been previously reported [70]. These
290 neuroblasts express the normal neuroblast marker Deadpan (Dpn) (Fig. 7A-A''), but produce
291 few progeny, and some neuroblasts are present in the deep layers which would normally be
292 occupied by neuronal progeny. A large fraction of these neuroblasts in the central domain don't
293 express E(spl)mγGFP, a Notch signaling reporter [61], while all neuroblasts in the control regions
294 express E(spl)mγGFP (Fig. 7A-A''). Thus, Notch signaling is largely lost in cell-cycle arrested
295 neuroblasts.

296

297 **The role of cell cycle progression in the medulla TTF cascade.**

298 Next, we tested whether blocking cell-cycle progression also affected the medulla TTF cascade
299 progression. In *vsxGal4>PCNA RNAi* brains, neuroblasts in the affected region do not express
300 either Ey or Slp1/2, but keep expressing SoxN (Fig. 7B-C''). This suggests that an earlier

301 temporal transition step is blocked which is required for Ey expression, and this prevents us
302 from examining whether the Ey to Slp transition also requires cell cycle progression. To
303 circumvent this problem, we used the *ay*Gal4 to drive *UAS-DCR2* and PCNA RNAi. By adjusting
304 heat shock timing to induce clones, we were able to obtain a condition where Ey expression is
305 minimally affected, and at this condition we observed that Slp2 expression is still severely
306 delayed (Fig. 7E-E'''). In addition to the timing of clone induction, the *ayGal4* is also likely to be
307 weaker than VsxGal4 at inducing RNAi, and the cell cycle is likely only slowed down rather than
308 arrested when using *ayGal4*, because there are still some progeny produced in such clones.
309 Furthermore, Slp1/2 expression is also delayed when we knock down String /Cdc25 required for
310 the G2 to M phase transition[71], or overexpress Dacapo (Dap, a Cyclin-dependent kinase
311 inhibitor in the CIP/KIP family)[72] using *ayGal4* (Supplementary Figure S3A-B''). Thus, cell cycle
312 progression is also required for the precise timing of Ey to Slp1/2 transition.
313
314 **<u>Notch signaling can rescue Slp expression delay caused by cell cycle defects.</u>**
315 Finally, we tested if supplying Notch signaling to cell-cycle arrested or delayed neuroblasts can
316 rescue the timing of Slp expression initiation. We supplied active Notch in neuroblasts using a
317 *dpn>FRT-stop-FRT3-FRT-NICD* transgene (which drives the expression of NICD from the *dpn*
318 enhancer in presence of heat shock activated Flippase; see Methods), while simultaneously
319 inducing knockdown of PCNA using ayGal4 under the same heat shock condition that leaves Ey
320 expression largely unaffected. Supplying NICD was sufficient to rescue Slp2 expression in PCNA
321 RNAi clones (Fig. 7E-E'''). This suggests that for the Ey to Slp transition, the presence of active
322 Notch signaling can substitute for the requirement for the cell-cycle progression.

323

324 ## Discussion

325 **Evidence of direct transcriptional activation in the medulla TTF cascade.**

326

327 *Drosophila* neuroblasts are temporally patterned by sequentially expressed TTFs. Although the
328 expression pattern and mutant phenotypes suggest that TTFs form a transcriptional cascade,
329 direct transcriptional regulation between TTFs has not been demonstrated in most cases. This
330 work has characterized two enhancers of the *slp* genes that enable the expression of Slp1 and
331 Slp2 in medulla neuroblasts. The u8772 220bp enhancer is activated at an earlier stage relative
332 to the d5778 850bp enhancer. The d5778 850bp enhancer also seems to drive Slp2 expression
333 in surface glial cells ensheathing the medulla neuroblasts. In these two enhancers, we identified
334 sites for the previous TTF -Ey and Scro-a TTF expressed at around the same time as Slp1[16,17].
335 Deleting either enhancer alone did not eliminate the expression of endogenous Slp1 and Slp2,
336 suggesting that they act redundantly with one another and possibly with other enhancers active
337 in this context. Using GFP reporter assays, we have shown that mutation of Ey binding sites in
338 these enhancers abolishes reporter expression similar to genetic experiments where we
339 observe a loss of GFP reporter within *ey* RNAi clones. Our results are also consistent with
340 previous studies that showed a complete loss of endogenous Slp1/2 expression in *UAS-ey-RNAi*
341 expressing neuroblasts [19]. We also confirmed the *in vivo* binding of Ey to the identified
342 enhancers of Slp by Dam-ID sequencing. The expression of the TTF Scro is initiated
343 simultaneously as Slp1/2, and it has been shown that loss of Scro significantly reduces Slp
344 expression level[17]. Mutation of most probable Scro binding sites on the u8772 220bp enhancer
345 led to a complete loss of GFP reporter expression. In contrast, a similar manipulation of the

346 d5778 850bp enhancer led to a decreased intensity of GFP reporter expression but did not
347 eliminate it. Thus the combined effect of mutating Scro binding sites on both enhancers
348 recapitulates the observed impact of Scro knock-down on endogenous Slp1/2 expression, which
349 is reduced expression of Slp1/2 in neuroblasts expressing *UAS scro-RNAi* and a consequent loss
350 of neural fates specified by Slp1/2 in their progeny. The observed differences in effects of Scro
351 binding site mutation on the two enhancers also highlights a general feature of enhancer
352 redundancy in fine-tuning expression of developmentally regulated genes- that different
353 enhancers are often sensitive to different environmental signals [49], which ultimately helps in
354 ensuring robust gene expression if an important regulator is absent or is present but at
355 insufficient concentrations for enhancer activation. It is also interesting to note that our
356 observation of multiple enhancers regulating Slp1/2 expression is consistent with regulation of
357 Slp1/2 in other developmental contexts. Previous studies have noted the presence of multiple
358 enhancers of Slp1/2 expression in the vicinity of the *slp1* and *slp2* coding loci . Many of these
359 regulatory DNA segments function as stripe enhancers enabling Slp1/2 to function as pair-rule
360 genes during embryonic segmentation[50]. Though these enhancers share some overlapping
361 functions and domains of activation, a full complement of stripe enhancers is required for
362 maintaining parasegment boundaries and wingless expression [74, 50].
363

364 **<u>Notch signaling directly regulates transcription of a temporal patterning factor</u>**

365 It was previously demonstrated that although Ey is necessary for activating Slp1/2 expression it
366 is not sufficient [19]. There is always a time delay after the start of Ey expression to the start of Slp
367 expression to ensure the sufficient duration of the Ey window. How is the timing controlled?

368 From our analyses of the *slp1/2* enhancer sequences we found several binding sites for the CSL
369 transcription factor Su(H), most prominently known as a central component of the ternary
370 Notch transcription complex and the primary DNA binding component. To confirm the
371 involvement of the Notch pathway in regulating Slp1/2, we observed effects of knocking down
372 key Notch pathway components on endogenous Slp1/2 expression. In all cases we observed a
373 delay in expression of Slp1/2 in neuroblasts expressing the RNAi knockdowns compared to the
374 time of Slp1/2 initiation in wild type neuroblasts. Mutating Su(H) binding sites in the u8772
375 220bp and the d5778 850bp enhancers led to a loss or delay of GFP reporter expression in
376 neuroblasts. These results suggest that the u8772 220bp and the d5778 850bp enhancers are
377 sensitive to Su(H) and further support the role of the Notch pathway in regulating the timing of
378 Slp1/2 expression. However, Ey may still play a more central role in activating Slp1/2 expression
379 than the Notch pathway since Slp1/2 are still expressed albeit later in the absence of Su(H) and
380 other Notch components. As with Ey, we confirmed Su(H) binding to our enhancers of interest
381 using DamID-seq. Thus, our work provided strong evidence that N signaling, a general signaling
382 pathway involved in neuroblast development, regulates the timing of activation of a TTF gene.
383 This might be part of mechanisms to promote TTF cascade progression specifically in
384 neuroblasts, where Notch signaling is active.
385

386 **<u>Cooperative regulation of target genes including *slp* by the TTF Ey and Notch signaling</u>**

387 What might explain the delay in Slp1/2 expression in the absence of Notch function? Recent
388 developments of single-molecule Fluorescence In Situ Hybridization (smFISH) technology and
389 live imaging techniques using the MS2-MCP system have enabled studying the transcription

390 process in molecular detail. Imaging transcription driven by Notch responsive enhancers in
391 native contexts has shown this process to be inherently 'bursty', i.e., episodes of transcription
392 (enhancer 'On' state) are punctuated with gaps in activity (enhancer in 'Off' state) [75,76]. The
393 dosage of NICD modulates the duration of the 'On' phase in one context studied by live imaging
394 [75,76]. Additionally, binding of tissue-specific regional factors to these Notch responsive
395 enhancers may prime these enhancers and help synchronize transcription and sustain a steady
396 transcriptional output upon Notch binding to enhancers; this helps integrate important
397 positional cues and the perception of context [75]. Applying these insights to our system, we
398 suggest that the delay observed may correspond to an increased number of abortive
399 transcription events in the absence of Su(H) and Notch and in the presence of Ey alone. Ey may
400 also act by priming our Notch responsive enhancers providing crucial contextual information
401 before robust levels of Slp1/2 can be transcribed, in addition to its independent role in helping
402 initiate Slp1/2 expression. The possible role of Ey in providing specificity to Notch mediated
403 regulation is supported by observations from our DamID data that 62.78% of Su(H) bound
404 genes and 60.3% of Ey bound genes were also bound by the other transcription factor. Enriched
405 GO terms within genes bound by both Ey and Su(H) included 'Notch signaling', 'asymmetric cell
406 division', 'cell division', 'apical cell polarity', 'axon guidance' etc (Fig 6C-H).

407 **<u>The role of cell cycle progression and Notch signaling in the medulla TTF cascade</u>**

408 Notch targeting genes and Dpn are transcriptional repressors that act partially redundantly to
409 maintain neuroblast identity. In type II NBs, Dpn is dependent on Notch signaling, and loss of
410 Dpn causes premature differentiation[37,77]. However, in type I NBs, Dpn is not lost when N
411 signaling is lost, and N signaling seems dispensable for the self-renewing abilities of NBs[39-41]. In

412 the medulla neuroblasts, we also observed that in *Su(H)* mutant clones, the clone size and
413 neuroblast prolifeation is not significantly affected. On the other hand, we observed that N
414 signaling is dependent on cell-cycle progression, and N target gene is lost when cell cycle
415 progression is blocked.
416 In the medulla, blocking cell cycle progression in neuroepithelial cells prematurely transform
417 them into neuroblasts, and these neuroblasts seem to be arrested in the TTF cascade at the
418 SoxN stage. The expression of Ey and Slp are never turned on in such neuroblasts. When we
419 arrested or slowed down the cell cycle later in neuroblasts to preserve Ey expression, we
420 observed Slp expression is still delayed. Therefore, cell cycle progression also has a role in the
421 Ey to Slp transition. Further we showed that supplying Notch signaling is sufficient to rescue the
422 delay in the Ey to Slp transition caused by cell cycle defect. Thus at the Ey to Slp transition, the
423 cell cycle effect is mediated through the direct regulation of Slp transcription by Notch
424 signaling. Taken together, our results suggest that in Ey stage neuroblasts, Ey is required to
425 initiate Slp expression but not sufficient to activate it to a strong level right away, and after
426 each asymmetric division, activation of Notch signaling in the neuroblast enhances Slp
427 expression, until Slp expression reaches a certain level to repress Ey expression and make the
428 transition. This can be part of a mechanism to coordinate the TTF temporal transition with the
429 cell cycle progression in order to generate the appropriate number of neural progeny at a given
430 temporal stage.

431 ## Methods

432 **Fly stocks and genetics**

433 Flies were reared on yeast food at 25°C unless otherwise stated.

434 Enhancer identification- Flies carrying the *GMR35H02-Gal4* insertion (BDSC 49923) were
435 crossed with transgenic flies expressing *UAS GFPnls* (BDSC 4776). GFP driven by the *GMR35H02-*
436 *Gal4* was then compared to endogenous Slp1 and Slp2 expression. Procedure for making
437 transgenic constructs and strains is described separately.

438 RNAi experiments- The following RNAi lines were used for RNAi knockdown experiments (In Fig
439 2); *UAS-ey-RNAi* (BDSC 32486), *UAS-scro*^{RNAi} (BDSC 33890), *UAS-N-RNAi* (BDSC 7078), *UAS-*
440 *Su(H)-RNAi* (VDRC 103597), *UAS-Dl-RNAi* (VDRC 32788), *UAS-PCNA-RNAi* (VDRC 51253), *UAS-*
441 *stg-RNAi* (VDRC 17760).

442 *ayGal4* (*actin*>FRT-y^{+}-STOP-FRT-Gal4, in which *actin* promoter drives Gal4 expression after a
443 STOP cassette is excised by the action of heat shock activated Flippase) was used to drive RNAi
444 of *ey*, *scro* and *su(h)*. Flies of genotype *ywhsFlp; ayGal4>UAS GFP; UAS Dcr2/Tm6B* were crossed
445 to the RNAi lines. Larvae were heat shocked at 37°C for 10 minutes 48 hours after egg laying
446 and then raised at 29°C, until brains of third instar larvae were dissected and stained.

447 For observing effect of *ey RNAi* on the GFP reporter expression (Fig 3) flies of genotype *ywhsFlp;*
448 *ayGal4>UAS lacZ; eyRNAi* (made by combining *ayGal4>UAS lacZ* on chromosome II (BDSC 4410)
449 with *UAS-ey RNAi* on chromosome III) were crossed to flies with genotype *ywhsFlp; Sp/CyO;*
450 *u8772 220bp>GFP* (enhancer1) or *ywhsFlp; Sp/CyO; d5778 870bp>GFP* (enhancer2).

451 For studying effects of *Su(H) RNAi* on GFP reporter expression, flies of genotype *ywhsFlp;*
452 *ayGal4>lacZ; Tm2/Tm6B* were crossed to flies of genotype *Dcr2; Su(H) RNAi; u8772 220>GFP*
453 (enhancer 1) or *Dcr2; Su(H) RNAi; d5778 870> GFP* (enhancer 2).

454 Heat shock protocols for RNAi experiments driven by *ayGal4* in presence of GFP reporters were
455 the same as described above for *ayGal4* driven RNAi by themselves (i.e., without GFP
456 reporters).

457 Cell cycle arrest experiments- For some experiments examining effect of cell cycle arrest on
458 Slp1/2 expression and on expression of the Notch reporter E(spl)-mγ::GFP, *VsxGal4* was used to
459 drive the expression of *UAS PCNA RNAi* and *UAS Dcr2* in neuroblasts. Flies of genotype *VsxG4;*
460 *E(spl)-mγGFP;UAS Dcr2/Tm6B* were crossed to those with genotype *ywhsFlp; UAS-PCNA RNAi*.
461 Larvae were shifted to 29°C 48 hours after egg laying. Brains of third instar larvae were
462 observed. For other experiments, flies of genotype *ywhsFlp; UAS-PCNA RNAi* were crossed to
463 flies of genotype *ywhsFlp; ayGal4>UAS GFP; UAS Dcr2/Tm6B*. Larvae with genotype *ywhsFLP;*
464 *ayGal4UASGFP /UAS-PCNARNAi; UASDCR2/+* were heat shocked for 8 minutes at 37°C 50 hours
465 after egg laying (70 hours before they develop into climbing third instar larvae) and were then
466 dissected. For rescuing Notch expression in cell cycle arrested neuroblasts flies of genotype
467 *ywhsFlp; ayGal4>UAS GFP; UAS Dcr2/Tm6B* were crossed to those with genotype *ywhsFlp; UAS*
468 *PCNA RNAi; dpn>hsNICD*. Larvae of genotype *ywhsFLP; ayGal4UASGFP /UAS-PCNARNAi;*
469 *UASDCR2/dpn>hsNICD* were then heat shocked for 8 minutes at 37°C 50 hours after egg laying
470 (70 hours before the third instar stage) as before and then dissected.

471 Negative labeling of *slp* loss of function clones- *UbiFRT40ARFP/CyO* flies (BDSC 34500) were
472 crossed with flies of genotype *ywhsFlp;Sp/CyO; u8772 220bp>GFP* (enhancer1) and *ywhsFlp*
473 *;Sp/CyO; d5778 870bp>GFP* (enhancer2) to create strains with genotypes *ywhsFlp;*
474 *Ubi>RFPFRT40A; u8772 220bp>GFP* and *ywhsFlp; Ubi>RFPFRT40A; d5778 870bp>GFP*
475 respectively. Flies of genotype *ywhsFlp; SlpS37A/Sm6-Tm6B* flies (a kind gift from Dr. Andrew

476 Tomlinson) were then crossed to *ywhsFlp; Ubi>RFPFRT40A; u8772 220bp>GFP* and *ywhsFlp;*
477 *Ubi>RFPFRT40A; d5778 870bp>GFP* and larvae were heat shocked for 45 minutes 48 hours after
478 egg laying. Third instar larvae were then dissected. The *ywhsFlp; SlpS37A/Sm6-Tm6B* strain
479 carries a deletion on chromosome II that spans both Slp1 and Slp2 genes. Clones carrying two
480 copies of this deficiency are seen as dark regions amidst Ubi>RFP marked wild type neuroblasts.

481 **Bioinformatic identification of TFBS**

482 Initially, to identify a list of possible candidate TFs with binding sites within our enhancers we
483 analyzed our enhancer sequences using the MEME suite tools[78] and TOMTOM[79] and the also by
484 an analytic tool developed at EPFL (https://biss.epfl.ch) that uses FIMO[80] to identify motifs on a
485 sequence (Michael Frochaux, Dr.Bart Deplancke personal communication) to complement our
486 findings from TOMTOM. However mutating sites identified by this initial round of analysis did
487 not always result in GFP reporter expression patterns that were consistent with our
488 observations from the genetic experiments (data not shown). We suspected this could be
489 because these analyses may have not exhaustively identified all potential binding sites for our
490 regulators. To this end we employed a slightly different strategy to identify all possible binding
491 sites of Ey, Su(H), and Scro whose knockdown had affected the expression of GFP reporters in
492 genetic experiments. We searched for consensus motifs of transcription factor binding sites for
493 Ey, Su(H), Slp1 in JASPAR[81,82] and Fly Factor Survey[83] and then searched for potential matches to
494 these consensus sequences in our enhancers using the DNA Pattern Recognition program in
495 Sequence Manipulation Tool[65]. Since consensus motifs for Scro binding sites were not
496 annotated in either JASPAR or Fly Factor Survey we instead picked 20 related transcription
497 factors of the NK-domain TF family whose consensus binding motifs were annotated (listed in

498 Supplementary Table 2). We looked for potential matches to these motifs within our enhancers
499 using the Pattern Recognition Tool of the Sequence Manipulation Suite. Sequences that were
500 most shared between the 20 NK domain containing TFs we examined were scored as the most
501 likely motifs for Scro binding in the d5778 870bp enhancer. Given the smaller size of the u8772
502 220bp enhancer, only motifs corresponding to Vnd binding sites were mutated since Scro has
503 been suggested to share the greatest homology to vnd of all other NK domain containing TFs[55].

504 **Plasmids constructs and making transgenic fly stocks**

505 Primer sequences for all cloning are provided in a supplementary table (Supplementary Table
506 2).

507 For making all constructs DNA was amplified from template using Expand High-Fidelity
508 Polymerase (Roche) unless stated otherwise and all constructs were verified by sequencing. All
509 fly embryo injections for making transgenic flies were carried out by Bestgene Inc, Chino Hills,
510 CA.

511 Generating constructs for reporter assays and enhancer bashing and making transgenic
512 reporter expressing stocks- Sequences corresponding to the fragments of regulatory DNA
513 encoded in GMR35H02 and the d5778 REDfly enhancer were cloned from the BAC clone CH321-
514 94O18[84] (BACPAC resources). Sequences were PCR amplified from this BAC and cloned into
515 pJR12 vector (a kind gift from Dr. Jens Rister) between *AscI* and *NotI* sites. Transgenes were
516 inserted at the landing site VK00027 on the third chromosome (BL9744) by ϕC31 integrase
517 mediated transgenesis[85] and positive transformants were screened using the w+ marker
518 originally present in the pJR12 plasmid. Mutated enhancers were custom synthesized as gene

519 blocks (gBlocks,IDT DNA) and cloned as stated above. Split gBlocks were custom made for
520 making the d5778 ey site mutant and the d5778 su(h) site mutants. These split gBlocks were
521 then PCR spliced and cloned between NotI and AscI sites of the pJR12 vector. A custom-made
522 gBlock was used for making the d5778 scro mutant reporter. All reporters were integrated at
523 the same genomic site to ensure comparability across constructs and experiments.

524 Generation of CRISPR enhancer deletion constructs and transgenic stocks- CRISPR gRNAs were
525 designed by entering sequences of genomic DNA of the target +/- 20 kbp into the CRISPR
526 Optimal Target Finder web utility [86] (https://www.targtfinder.flycrispr.neuro.brown.edu). Four
527 gRNAs-two upstream and two downstream of the target region to be deleted were then
528 selected. All four gRNAs were then cloned into the vector pCFD5[87] (Addgene plasmid #73914 a
529 kind gift from Dr. Simon Bullock) using NEB-Builder HiFi DNA Assembly master mix. Constructs
530 were then injected into fly strain containing *M{nos-cas9}ZH-2A* (BL54591) along with a 120 bp
531 repair oligonucleotide that contained 60bp of wild type genome sequence flanking both ends of
532 the expected double-stranded break. After injection, the *nos-cas9* source was eliminated in the
533 subsequent generations by crossing individual G0 progeny flies to a double balancer of
534 genotype *ywhsFlp; Sp/CyO; Tm2/Tm6B* and selecting male G1 progeny. Individual G1 males
535 were then crossed to the same double balancer line to create stocks. The G1 males were then
536 genotyped by PCR to identify whether their genome had been edited, using RedExtract-n-Amp
537 tissue PCR kit (Sigma-Aldrich). G2 progeny of genome-edited males were then raised until
538 homozygous stocks were established.

539 Generation of the heat shock inducible NICD construct: We modified the pJR12 vector used in
540 enhancer bashing experiments to replace the GFP coding sequence with coding sequences of

541 our interest. First, we generated a DNA fragment that matched the sequences of the pJR12
542 vector flanking the eGFP sequence but that did not contain the eGFP sequence itself by PCR
543 splicing. We then cut-out the eGFP segment from the pJR12 vector and replaced it with our GFP
544 deleted fragment using *NsiI* and *XhoI*. Next, an *FRT-stop-FRT3-FRT* segment was cloned from
545 the CoinFlp plasmid[88] (Addgene plasmid # 52889, a kind gift from Dr. Iswar Hariharan) and PCR
546 spliced with a fragment of Notch Intracellular Domain (NICD). Sequences corresponding to the
547 Notch Intracellular Domain were PCR amplified from Notch cDNA LD34134 (DGRC). The *FRT-*
548 *stop-FRT3-FRT-NICD* fragment was then cloned into the modified pJR12 vector between the
549 *PmeI* and *AgeI* restriction sites. The deadpan enhancer sequence amplified from the BAC clone
550 CH321-86A18 (BACPAC resources) was then cloned into the modified pJR12 vector to drive the
551 heat shock inducible NICD expressing construct in presence of a heat shock activated Flippase
552 or *hsFlp* (this construct is abbreviated as *dpn> hsNICD*). Construct was inserted at the VK00027
553 landing site (BL 9744) by ϕC31 integrase mediated transgenesis. Positive transformants were
554 identified by the w+ eye color marker expression and stocks were created by crossing to a
555 double balancer of genotype *ywhsFlp; Sp/CyO; Tm2/Tm6B*.

556 <u>Generation of DamID-fusion constructs (*UAS Dam-Ey* and *UAS-Dam-Su(H)*) and transgene</u>
557 <u>expressing stocks</u>- Su(H) coding sequence was amplified from a cDNA clone GH10914 (DGRC) by
558 PCR. The amplified Su(H) coding sequence was cloned into the pUAST-Dam-attB vector[67] (a kind
559 gift from Dr. Andrea Brand) between the *NotI* and *XhoI* sites. A gBlock of Ey coding sequence
560 was ordered from IDT and cloned into the pUAST-Dam-attB vector. Constructs were then
561 incorporated at the VK00027 landing site (BL 9744) by ϕC31 mediated integration.

562 Transformants were identified by expression of the w+ marker gene. Final stocks were
563 established by crossing to a double balancer line of genotype *ywhsFlp; Sp/CyO; Tm2/Tm6B*.

564 **Immunofluorescence staining**

565 Antibody staining was carried out as described in [19] with a few modifications. The protocol is
566 described briefly as follows: brains from climbing third instar larvae were dissected in 1XPBS
567 and fixed in 4% Formaldehyde solution in 1X PBS for 30 minutes on ice. Brains were then
568 incubated in primary antibody solution overnight at 4°C, washed three times for 30 minutes
569 each at 4°C, then incubated in fluor conjugated- secondary antibody solution overnight at 4°C
570 and then washed again thrice at room temperature each time for 30 minutes. Samples were
571 mounted in Slowfade Gold antifade reagent (Invitrogen). Images are acquired using a Zeiss
572 LSM500 Confocal Microscope.

573 Antibodies used in the study are as follows: rabbit anti-Slp1, guinea-pig anti-Slp2, rabbit anti-Ey
574 (all used at 1:500) were kind gifts from Dr. Claude Desplan, guinea-pig anti-Dpn (1:500) (a kind
575 gift from Dr. Chris Doe). Commercially available antibodies include - sheep anti-GFP (1:500,
576 AbD Serotec, 4745-1051), Chicken anti-beta-gal (1:500, Abcam ab9361), Rat anti-Deadpan
577 [11D1BC7] (1:200, Abcam, ab195173) mouse anti-PCNA (1:50, Abcam ab29). These antibodies
578 are provided by the Developmental Studies Hybridoma Bank (DSHB): mouse anti-eyeless (1:10),
579 mouse anti-Pros (MR1A 1:20). Secondary antibodies are from Jackson or Invitrogen.

580 **Fluorescence In situ hybridization (FISH)**

581 FISH was carried out using custom made Stellaris probe sets as described in [89] except that
582 incubation with sodium borohydride was skipped. Probes were generated using the slp1 mRNA

583 and slp2 mRNA as templates. Concurrent FISH and immunofluorescence staining was carried
584 out as described in the same publication.

585 **DamID-Seq**

586 Flies of genotype *ywhsFlp; Sp/CyO; UAS-Dam/ Tm6B, ywhsFlp; Sp/CyO; UAS-Ey-Dam/ Tm6B* or
587 *ywhsFlp; Sp/CyO; UAS-Su(H)-Dam /Tm6B* were crossed with *Dcr2; tubG80ts; SoxNGal4*. Mating
588 crosses were incubated at 25 °C. Eggs laid within an 8-hour window were then shifted to 18°C
589 for 3 days until they hatched. The expressions of the Dam-fusion proteins were then induced in
590 larval brains by shifting the larvae to 29°C for 72 hours. Climbing third instar larvae were then
591 dissected. Only the optic lobes were used for further sample preparation. For each sample
592 around 100 brains were dissected.

593 Dam-ID libraries were made as described in [90]. Briefly, fly brains were dissected in 1X PBS and
594 genomic DNA was isolated using QIAamp DNA Micro kit (Qiagen). Genomic DNA was then
595 digested with DpnI and purified using spin column purification (Qiagen PCR-purification kit). To
596 the DpnI digested DNA DamID-PCR adaptors were ligated. Subsequently the adaptor ligated
597 DNA fragments were digested with DpnII. The DpnII digested genomic DNA fragments were
598 then amplified by PCR to enrich for bound GATC fragments. To make sequencing libraries the
599 PCR enriched genomic DNA sample was sonicated using a Bioruptor bath sonicator
600 (Diagenode), purified using AMPure XP beads, end-repaired and 3'-adenylated. Illumina
601 sequencing indexes were then ligated to these fragments. Index-labeled DNA fragments were
602 then further enriched by PCR amplification, checked for quality and fragment size distribution
603 on an Agilent Bioanalyzer and by qPCR (Quality control of all libraries was carried out at the

604 Functional Genomics Unit of Roy J. Carver Biotechnology Center, UIUC). Libraries that were
605 deemed acceptable were then sequenced on a single SP100 lane of an Illumina NovaSeq
606 sequencer. Read lengths were 100bp. Two Biological replicates each of *Ey-Dam*, *Su(H)-Dam* and
607 *Dam*-only samples were sequenced, and each biological replicate is defined as one library
608 generated from ~100 dissected brains. Number of reads obtained were as follows: Dam
609 replicate1: 53745480 reads, Dam replicate 2: 85637355 reads, Ey-Dam replicate 1: 81121107
610 reads, Ey-Dam replicate 2: 82085708 reads, SuH-Dam replicate 1: 77448608 reads, replicate 2:
611 80015207 reads. All samples exhibited good QC scores.

612 **DamID-Seq data analysis**

613 DamID-seq data was analyzed using the damidseq-pipeline [91]. Duplicate samples of Ey-Dam and
614 Su(H)-Dam samples and Dam-only controls were aligned to the Drosophila reference genome
615 UCSC dm6. Alignment rate for individual samples were as follows:(Ey-Dam replicate 1- 97.04%,
616 Ey-Dam replicate 2 -97.82%, Su(H)-Dam replicate 1- 97.91% and Su(H)-Dam replicate 2 –
617 97.82%. The main utility- the damid-seqpipeline was used to align reads to the genome using
618 bowtie2, bin and count reads, normalize counts and generate log-2 ratio bedgraph files for each
619 DamID-sample and its corresponding Dam-only control. The provided gatc.track file was used
620 for running the script. Next, the findpeaks utility was used with an F.D.R. <0.01 to identify
621 peaks. We then used the provided peaks2genes utility to assign peaks to genes. To assess the
622 reproducibility of our data we also ran the findpeaks script using F.D.R <0.1 to discover peaks
623 with weaker statistical confidence and used this as input for the I.D.R. Python package
624 (https://github.com/nboley/idr). 984 of 1810 (54.4.%) Ey-Dam and 972 of 1996 (48.7%) of
625 Su(H)-Dam peaks passed an I.D.R. threshold of 0.05. Lists of genes bound reproducibly by both

626 Ey-Dam and by Su(H)-Dam were used in BioVenn[92] to visualize the overlap between these two
627 lists and estimate percentage of genes regulated by both transcription factors. Enriched gene
628 ontology terms in this list were identified using DAVID [93,94]. All replicate tracks for Ey and for
629 Su(H) as well as reproducible peaks identified using I.D.R. were visualized in IGV [95].

630 **Image quantification and statistical analysis.**

631 No statistical method was used to predetermine sample size. Sample size /replicate numbers
632 were decided based on routine in the field and previous experience. All data were obtained
633 from at least two independent experiments. The numbers of animals or clones analyzed can be
634 found in figure legends or this section (see below). All data are highly reproducible. No outliers
635 are excluded. For specific quantification method and statistical analysis see below.

636 Imaging and image analysis for comparison of wild type and mutant GFP reporter intensities- All
637 images were acquired using a Zeiss LSM 500 confocal microscope. Samples were imaged at sub-
638 saturating illumination conditions, with stack intervals of 1 micron. Same laser settings and
639 imaging conditions were used across all variants of the same enhancers. Image analysis was
640 carried out using Fiji [96]. Signal intensities in the GFP and the Dpn channels were measured over
641 a small rectangular selection for all variants. For the same enhancer a 'scaling factor' was
642 calculated for each mutant by dividing the Dpn channel intensity for mutant reporter by the
643 channel intensity of the corresponding wild type reporter. The GFP channel intensities for each
644 variant was then multiplied by this scaling factor. Finally a ratio of the scaled GFP channel
645 intensity to the Dpn channel intensity was calculated for each GFP reporter variant. Ratios of
646 scaled GFP/Dpn intensities was then plotted using GraphPad Prism and for each enhancer RM

One-way ANOVA with Geisser-Greenhouse correction and Tukey's multiple comparisons were carried out between reporter variants of the same enhancer. For the d5778 870bp enhancer five sets of data from twenty different optic lobes were acquired for each enhancer (one set- wild type and all mutant variations all imaged using the same conditions). For the u8772 220bp enhancer six sets of data were used for quantification.

Image analysis for CRISPR enhancer deletion experiments- All images were acquired using a Zeiss LSM 500 confocal microscope under sub-saturating illumination conditions. For each sample width of Slp1, Slp2 and Dpn expression domains was measured in Fiji at five different locations and averaged. The brain size of the sample was estimated by measuring the length of the brain at its widest point perpendicular to the neuroblast division axis. The width of each protein expression domain was divided by the brain size to normalize expression domain size estimates to the brain size. For each protein Slp1, Slp2 and Dpn- these ratios were then plotted in GraphPad Prism and ordinary one way ANOVA and Dunnett's multiple comparisons tests were carried out between wild type and CRISPR enhancer deleted brains. Data from seven brains of each genotype was analyzed and quantified.

All images were processed in Adobe Photoshop and assembled using Adobe Illustrator.

Data Availability

The raw and processed DamID-seq data have been deposited to GEO, and the accession number is GSE188643 (reviewer's token qncnwyyidtsndcp).

Acknowledgments

667 We thank the Functional Genomics Unit and the DNA-Sequencing Services Unit of the Roy J.
668 Carver Biotechnology Center at the University of Illinois at Urbana-Champaign for assistance with
669 quality control and sequencing of Dam-ID sequencing libraries. We thank the fly community,
670 especially Claude Desplan, Andrea Brand, Chris Doe, Bruce Edgar, Kenneth Irvine, Miki Fujioka
671 and James B. Jaynes for generous gifts of antibodies and fly stocks. We are grateful to Bart
672 Deplancke' team for help with the YIH pipeline to predict transcription factor binding sites within
673 enhancers. We thank the Bloomington Drosophila Stock Center, the Vienna Drosophila RNAi
674 Center, the Developmental Studies Hybridoma Bank, and TriP at Harvard Medical School
675 (NIH/NIGMS R01-GM084947) for fly stocks and reagents. We thank members of the Li lab Dr. Yu
676 Zhang and Hailun Zhu for helpful discussions. This work was supported by the National Eye
677 Institute (Grant 1 R01 EY026965-01A1) and start-up funds from the University of Illinois at
678 Urbana-Champaign.

679 **Competing interests.**

680 The authors declare no competing or financial interests.

681 **Materials & Correspondence.** Publicly available fly lines (those from BDSC or VDRC) should be
682 requested directly from the corresponding stock centers: https://bdsc.indiana.edu/ or
683 https://stockcenter.vdrc.at/control/main. Fly lines generated in this study can be requested
684 without restriction. Correspondence and requests for materials should be addressed to Xin Li
685 (lixin@illinois.edu).

686 **References**

687 1 Lin, S. & Lee, T. Generating neuronal diversity in the Drosophila central nervous system. *Dev Dyn*
688 **241**, 57-68, doi:10.1002/dvdy.22739 (2012).

689 2 Allan, D. W. & Thor, S. Transcriptional selectors, masters, and combinatorial codes: regulatory
690 principles of neural subtype specification. *Wiley Interdiscip Rev Dev Biol* **4**, 505-528,
691 doi:10.1002/wdev.191 (2015).
692 3 Holguera, I. & Desplan, C. Neuronal specification in space and time. *Science* **362**, 176-180,
693 doi:10.1126/science.aas9435 (2018).
694 4 Sagner, A. & Briscoe, J. Establishing neuronal diversity in the spinal cord: a time and a place.
695 *Development* **146**, doi:10.1242/dev.182154 (2019).
696 5 Pearson, B. J. & Doe, C. Q. Specification of temporal identity in the developing nervous system.
697 *Annu Rev Cell Dev Biol* **20**, 619-647, doi:10.1146/annurev.cellbio.19.111301.115142 (2004).
698 6 Oberst, P., Agirman, G. & Jabaudon, D. Principles of progenitor temporal patterning in the
699 developing invertebrate and vertebrate nervous system. *Curr Opin Neurobiol* **56**, 185-193,
700 doi:10.1016/j.conb.2019.03.004 (2019).
701 7 Maurange, C. Temporal patterning in neural progenitors: from Drosophila development to
702 childhood cancers. *Dis Model Mech* **13**, doi:10.1242/dmm.044883 (2020).
703 8 Doe, C. Q. Temporal Patterning in the Drosophila CNS. *Annu Rev Cell Dev Biol* **33**, 219-240,
704 doi:10.1146/annurev-cellbio-111315-125210 (2017).
705 9 Miyares, R. L. & Lee, T. Temporal control of Drosophila central nervous system development.
706 *Curr Opin Neurobiol* **56**, 24-32, doi:10.1016/j.conb.2018.10.016 (2019).
707 10 Brody, T. & Odenwald, W. F. Programmed transformations in neuroblast gene expression during
708 Drosophila CNS lineage development. *Dev Biol* **226**, 34-44, doi:10.1006/dbio.2000.9829 (2000).
709 11 Isshiki, T., Pearson, B., Holbrook, S. and Doe, C.Q. . Drosophila neuroblasts sequentially express
710 transcription factors which specify the tmporal identity of their neuronal progeny *Cell* **106**, 511-
711 521 (2001).
712 12 Grosskortenhaus, R., Robinson, K. J. & Doe, C. Q. Pdm and Castor specify late-born motor
713 neuron identity in the NB7-1 lineage. *Genes Dev* **20**, 2618-2627, doi:10.1101/gad.1445306
714 (2006).
715 13 Baumgardt, M., Karlsson, D., Terriente, J., Diaz-Benjumea, F. J. & Thor, S. Neuronal subtype
716 specification within a lineage by opposing temporal feed-forward loops. *Cell* **139**, 969-982,
717 doi:10.1016/j.cell.2009.10.032 (2009).
718 14 Li, X., Chen, Z. & Desplan, C. Temporal patterning of neural progenitors in Drosophila. *Curr Top*
719 *Dev Biol* **105**, 69-96, doi:10.1016/B978-0-12-396968-2.00003-8 (2013).
720 15 Suzuki, T., Kaido, M., Takayama, R. & Sato, M. A temporal mechanism that produces neuronal
721 diversity in the Drosophila visual center. *Dev Biol* **380**, 12-24, doi:10.1016/j.ydbio.2013.05.002
722 (2013).
723 16 Konstantinides, N. *et al.*, A comprehensive series of temporal transcription factors in the fly
724 visual system. Biorxiv (as accessed on 10/28/2021) doi:10.1101/2021.06.13.448242 (2021).
725 17 Zhu, H., Zhao, S. D., Ray, A., Zhang, Y. & Li, X., A comprehensive temporal patterning gene
726 network in Drosophila medulla neuroblasts revealed by single-cell RNA sequencing. Biorxiv (as
727 accessed on 10/28/2021) doi:10.1101/2021.06.12.448145 (2021).
728 18 Tang, J. L. Y. *et al.*, NanoDam identifies novel temporal transcription factors conserved between
729 the Drosophila central brain and visual system. Biorxiv (as accessed on 10/28/2021)
730 doi:10.1101/2021.06.07.447332 (2021).
731 19 Li, X. *et al.* Temporal patterning of Drosophila medulla neuroblasts controls neural fates. *Nature*
732 **498**, 456-462, doi:10.1038/nature12319 (2013).
733 20 Maurange, C., Cheng, L. & Gould, A. P. Temporal transcription factors and their targets schedule
734 the end of neural proliferation in Drosophila. *Cell* **133**, 891-902, doi:10.1016/j.cell.2008.03.034
735 (2008).

736 21 Averbukh, I., Lai, S. L., Doe, C. Q. & Barkai, N. A repressor-decay timer for robust temporal
737 patterning in embryonic Drosophila neuroblast lineages. *Elife* **7**, doi:10.7554/eLife.38631 (2018).
738 22 Hirono, K., Margolis, J. S., Posakony, J. W. & Doe, C. Q. Identification of hunchback cis-regulatory
739 DNA conferring temporal expression in neuroblasts and neurons. *Gene Expr Patterns* **12**, 11-17,
740 doi:10.1016/j.gep.2011.10.001 (2012).
741 23 Grosskortenhaus, R., Pearson, B. J., Marusich, A. & Doe, C. Q. Regulation of temporal identity
742 transitions in Drosophila neuroblasts. *Dev Cell* **8**, 193-202, doi:10.1016/j.devcel.2004.11.019
743 (2005).
744 24 Mettler, U., Vogler, G. & Urban, J. Timing of identity: spatiotemporal regulation of hunchback in
745 neuroblast lineages of Drosophila by Seven-up and Prospero. *Development* **133**, 429-437,
746 doi:10.1242/dev.02229 (2006).
747 25 van den Ameele, J. & Brand, A. H. Neural stem cell temporal patterning and brain tumour
748 growth rely on oxidative phosphorylation. *Elife* **8**, doi:10.7554/eLife.47887 (2019).
749 26 Okamoto, M. *et al.* Cell-cycle-independent transitions in temporal identity of mammalian neural
750 progenitor cells. *Nat Commun* **7**, 11349, doi:10.1038/ncomms11349 (2016).
751 27 Moore, R. & Alexandre, P. Delta-Notch Signaling: The Long and The Short of a Neuron's
752 Influence on Progenitor Fates. *J Dev Biol* **8**, doi:10.3390/jdb8020008 (2020).
753 28 Fortini, M. E. Notch signaling: the core pathway and its posttranslational regulation. *Dev Cell* **16**,
754 633-647, doi:10.1016/j.devcel.2009.03.010 (2009).
755 29 Kopan, R. & Ilagan, M. X. The canonical Notch signaling pathway: unfolding the activation
756 mechanism. *Cell* **137**, 216-233, doi:10.1016/j.cell.2009.03.045 (2009).
757 30 Bray, S. & Bernard, F. in *Notch Signaling Current Topics in Developmental Biology* 253-275
758 (2010).
759 31 Walsh, K. T. & Doe, C. Q. Drosophila embryonic type II neuroblasts: origin, temporal patterning,
760 and contribution to the adult central complex. *Development* **144**, 4552-4562,
761 doi:10.1242/dev.157826 (2017).
762 32 Knoblich, J. A., Jan Lily Y., and Jan Yuh Nung. Asymmetric segregation of Numb and Prospero
763 during cell division *Nature* **377**, 624-627 (1995).
764 33 Rhyu, M., S. , Jan, Lily, Y., and Jan Yuh Nung Asymmetric segregation of Numb protein during
765 division of the sensory organ precursor cell confers distinct fates to daughter cells. *Cell* **76**, 477-
766 491 (1994).
767 34 Roegiers, F. & Jan, Y. N. Asymmetric cell division. *Curr Opin Cell Biol* **16**, 195-205,
768 doi:10.1016/j.ceb.2004.02.010 (2004).
769 35 Fuerstenberg, S., Broadus, Julie, and Doe Chris, Q Asymmetry and cell fate in the Drosophila
770 embryonic CNS. *The International Journal of Developmental Biology* **42**, 379-383 (1998).
771 36 Wang, H. *et al.* Aurora-A acts as a tumor suppressor and regulates self-renewal of Drosophila
772 neuroblasts. *Genes Dev* **20**, 3453-3463, doi:10.1101/gad.1487506 (2006).
773 37 Bowman, S. K. *et al.* The tumor suppressors Brat and Numb regulate transit-amplifying
774 neuroblast lineages in Drosophila. *Dev Cell* **14**, 535-546, doi:10.1016/j.devcel.2008.03.004
775 (2008).
776 38 Weng, M., Golden, K. L. & Lee, C. Y. dFezf/Earmuff maintains the restricted developmental
777 potential of intermediate neural progenitors in Drosophila. *Dev Cell* **18**, 126-135,
778 doi:10.1016/j.devcel.2009.12.007 (2010).
779 39 Zacharioudaki, E., Magadi, S. S. & Delidakis, C. bHLH-O proteins are crucial for Drosophila
780 neuroblast self-renewal and mediate Notch-induced overproliferation. *Development* **139**, 1258-
781 1269, doi:10.1242/dev.071779 (2012).
782 40 Almeida, M. S. & Bray, S. J. Regulation of post-embryonic neuroblasts by Drosophila Grainyhead.
783 *Mech Dev* **122**, 1282-1293, doi:10.1016/j.mod.2005.08.004 (2005).

41 Magadi, S. S. *et al.*, doi:10.1101/2020.03.25.007187 (2020).
42 Ulvklo, C. *et al.* Control of neuronal cell fate and number by integration of distinct daughter cell proliferation modes with temporal progression. *Development* **139**, 678-689, doi:10.1242/dev.074500 (2012).
43 Bivik, C. *et al.* Control of Neural Daughter Cell Proliferation by Multi-level Notch/Su(H)/E(spl)-HLH Signaling. *PLoS Genet* **12**, e1005984, doi:10.1371/journal.pgen.1005984 (2016).
44 Kageyama, R., Ohtsuka, T., Shimojo, H. & Imayoshi, I. Dynamic regulation of Notch signaling in neural progenitor cells. *Curr Opin Cell Biol* **21**, 733-740, doi:10.1016/j.ceb.2009.08.009 (2009).
45 Pfeiffer, B. D., Jenett, A., Hammonds, A.S., Ngo, T. B., Misra, S., Murphy, C., Scully, A., Carlson, J. W., Wan, K.H., Laverty, T.R., Myngall, C., Svirkas, R., Kadonaga, J.T., Doe, C.Q., Eisen, M.B., Celniker, S.E., and Rubin, G.M. . Tools for neuroanatomy and neurogenetics in Drosophila *Proc Natl Acad Sci U S A* **105**, 9715-9720 (2008).
46 Jenett, A. *et al.* A GAL4-driver line resource for Drosophila neurobiology. *Cell Rep* **2**, 991-1001, doi:10.1016/j.celrep.2012.09.011 (2012).
47 Li, H. H. *et al.* A GAL4 driver resource for developmental and behavioral studies on the larval CNS of Drosophila. *Cell Rep* **8**, 897-908, doi:10.1016/j.celrep.2014.06.065 (2014).
48 Rister, J., Razzaq, A., Boodram, P., Desai, N., Tsanis, C., Chen, H., Jukam, D., and Desplan, C. . Single-base pair differences in a shared motif determine differential Rhodopsin expression. *Science* **350**, 1258-1261 (2015).
49 Frankel, N. *et al.* Phenotypic robustness conferred by apparently redundant transcriptional enhancers. *Nature* **466**, 490-493, doi:10.1038/nature09158 (2010).
50 Fujioka, M. & Jaynes, J. B. Regulation of a duplicated locus: Drosophila sloppy paired is replete with functionally overlapping enhancers. *Dev Biol* **362**, 309-319, doi:10.1016/j.ydbio.2011.12.001 (2012).
51 Ghiasvand, N. M. *et al.* Deletion of a remote enhancer near ATOH7 disrupts retinal neurogenesis, causing NCRNA disease. *Nat Neurosci* **14**, 578-586, doi:10.1038/nn.2798 (2011).
52 Lagha, M., Bothma, J. P. & Levine, M. Mechanisms of transcriptional precision in animal development. *Trends Genet* **28**, 409-416, doi:10.1016/j.tig.2012.03.006 (2012).
53 Gallo, S. M., Li, L., Hu, Z. & Halfon, M. S. REDfly: a Regulatory Element Database for Drosophila. *Bioinformatics* **22**, 381-383, doi:10.1093/bioinformatics/bti794 (2006).
54 Rivera, J., Keranen, S. V. E., Gallo, S. M. & Halfon, M. S. REDfly: the transcriptional regulatory element database for Drosophila. *Nucleic Acids Res* **47**, D828-D834, doi:10.1093/nar/gky957 (2019).
55 Zaffran, S., Das, G., and Frasch, M. . The NK-2 homeobox gene scarecrow (scro) is expressed in pharynx, ventral nerve cord and brain of Drosophila embryos. *Mechanisms of Development* **94**, 237-241 (2000).
56 Bailey, A. M. a. P., J. . Suppressor of Hairless directly activates transcription of enhancer of split complex genes in response to Notch receptor activity. *Genes and Development* **9**, 2609-2622 (1995).
57 Furukawa, T., Kobayakawa, Y., Tamura, K., Kimura, K., Kawaichi, M., Tanimura, T., and Honjo, T. . Suppressor of Hairless, the Drosophila homolog of RBP-Jkappa, transactivates the neurogenic gene E(spl)m8. *Japan Journal of Genetics* **70**, 505-524 (1995).
58 Ito, K., Awano, W., Suzuki, K., Hiromi, Y., and Yamamoto, D. The Drosophila mushroom body is a quadruple structure of clonal units each of which contains a virtually identical set of neurones and glial cells *Developemnt* **124**, 761-771 (1997).
59 Nusslein-Volhard, C., Wieschaus, E. and Kluding, H. . Mutations affecting the pattern of larval cuticle in Drosophila melanogaster I.Zygotic loci on the second chromosome *Roux's archives of developmental biology* **193**, 267-282 (1984).

832 60 Bray, S. J. Notch signalling: a simple pathway becomes complex. *Nat Rev Mol Cell Biol* **7**, 678-
833 689, doi:10.1038/nrm2009 (2006).
834 61 Campos-Ortega, J. A. Cellular interactions during early neurogenesis of Drosophila melanogaster
835 *Trends Neurosci* **11**, 400-405 (1988).
836 62 Fleming, R. J., Scottgale, T.N., Diederich, R.J., and Artavanis-Tsakonas, S. . The gene Serrate
837 encodes a putative EGF-like transmembrane protein essential for proper ectodermal
838 development in Drosophila melanogaster. *Genes Dev* **4**, 2188-2201 (1990).
839 63 Rebay, I., Fleming, R., Fehon, R.G., Cherbas, L., Cherbas, P., and Artavanis-Tsakonas, S. . Specific
840 EGF repeats of Notch mediate interactions with Delta and Serrate: Implicationsfor Notch as a
841 multifunctional receptor. *Cell* **67**, 687-699 (1991).
842 64 Kim, I. M., Wolf, M. J. & Rockman, H. A. Gene deletion screen for cardiomyopathy in adult
843 Drosophila identifies a new notch ligand. *Circ Res* **106**, 1233-1243,
844 doi:10.1161/CIRCRESAHA.109.213785 (2010).
845 65 Stothard, P. The sequence manipulation suite: JavaScript programs for analyzing and formatting
846 protein and DNA sequences *BioTechniques* **28**, 1102-1104 (2000).
847 66 van Steensel, B., and Henikoff, S. . Identification of in vivo DNA targets of chromatin proteins
848 using tethered Dam methyltransferase *Nature Biotechnology* **18**, 424-428 (2000).
849 67 Southall, T. D. *et al.* Cell-type-specific profiling of gene expression and chromatin binding
850 without cell isolation: assaying RNA Pol II occupancy in neural stem cells. *Dev Cell* **26**, 101-112,
851 doi:10.1016/j.devcel.2013.05.020 (2013).
852 68 Erclik, T. *et al.* Integration of temporal and spatial patterning generates neural diversity. *Nature*
853 **541**, 365-370, doi:10.1038/nature20794 (2017).
854 69 Moldovan, G. L., Pfander, B. & Jentsch, S. PCNA controls establishment of sister chromatid
855 cohesion during S phase. *Mol Cell* **23**, 723-732, doi:10.1016/j.molcel.2006.07.007 (2006).
856 70 Zhou, L. & Luo, H. Replication protein a links cell cycle progression and the onset of
857 neurogenesis in Drosophila optic lobe development. *J Neurosci* **33**, 2873-2888,
858 doi:10.1523/JNEUROSCI.3357-12.2013 (2013).
859 71 Edgar, B. A. a. O. F., P. Genetic control of cell division patterns in the Drosophila embryo. *Cell* **57**,
860 177-187 (1989).
861 72 Lane, M. E. *et al.* Dacapo, a Cyclin-Dependent Kinase Inhibitor, Stops Cell Proliferation during
862 Drosophila Development. *Cell* **87**, 1225-1235, doi:10.1016/s0092-8674(00)81818-8 (1996).
863 73 Prazak, L., Fujioka, M. & Gergen, J. P. Non-additive interactions involving two distinct elements
864 mediate sloppy-paired regulation by pair-rule transcription factors. *Dev Biol* **344**, 1048-1059,
865 doi:10.1016/j.ydbio.2010.04.026 (2010).
866 74 Cadigan, K. M., Grossniklaus,U., and Genring, W.J. . Localized expression of sloppy paired protein
867 maintains the polarity of Drosophila parasegments. . *Genes and Development* **8**, 899-913 (1994).
868 75 Falo-Sanjuan, J., Lammers, N. C., Garcia, H. G. & Bray, S. J. Enhancer Priming Enables Fast and
869 Sustained Transcriptional Responses to Notch Signaling. *Dev Cell* **50**, 411-425 e418,
870 doi:10.1016/j.devcel.2019.07.002 (2019).
871 76 Lee, C., Shin, H. & Kimble, J. Dynamics of Notch-Dependent Transcriptional Bursting in Its Native
872 Context. *Dev Cell* **50**, 426-435 e424, doi:10.1016/j.devcel.2019.07.001 (2019).
873 77 San Juan, B. P., Andrade-Zapata, I. & Baonza, A. The bHLH factors Dpn and members of the E(spl)
874 complex mediate the function of Notch signalling regulating cell proliferation during wing disc
875 development. *Biol Open* **1**, 667-676, doi:10.1242/bio.20121172 (2012).
876 78 Bailey, T. L., Johnson, J., Grant, C. E. & Noble, W. S. The MEME Suite. *Nucleic Acids Res* **43**, W39-
877 49, doi:10.1093/nar/gkv416 (2015).
878 79 Gupta, S., Stamatoyannopoulos, J. A., Bailey, T. L. & Noble, W. S. Quantifying similarity between
879 motifs. *Genome Biol* **8**, R24, doi:10.1186/gb-2007-8-2-r24 (2007).

880 80 Grant, C. E., Bailey, T. L. & Noble, W. S. FIMO: scanning for occurrences of a given motif.
881 *Bioinformatics* **27**, 1017-1018, doi:10.1093/bioinformatics/btr064 (2011).
882 81 Sandelin, A., Alkema, W., Engstrom, P., Wasserman, W. W. & Lenhard, B. JASPAR: an open-
883 access database for eukaryotic transcription factor binding profiles. *Nucleic Acids Res* **32**, D91-
884 94, doi:10.1093/nar/gkh012 (2004).
885 82 Fornes, O. *et al.* JASPAR 2020: update of the open-access database of transcription factor
886 binding profiles. *Nucleic Acids Res* **48**, D87-D92, doi:10.1093/nar/gkz1001 (2020).
887 83 Zhu, L. J. *et al.* FlyFactorSurvey: a database of Drosophila transcription factor binding
888 specificities determined using the bacterial one-hybrid system. *Nucleic Acids Res* **39**, D111-117,
889 doi:10.1093/nar/gkq858 (2011).
890 84 Venken, K. J. *et al.* Versatile P[acman] BAC libraries for transgenesis studies in Drosophila
891 melanogaster. *Nat Methods* **6**, 431-434, doi:10.1038/nmeth.1331 (2009).
892 85 Groth, A. C., Fish, M., Nusse, R., and Calos, M.P. . Construction of transgenic Drosophila by using
893 the site specific integrase from Phage PhiC31 *Genetics* **166**, 1775-1782 (2004).
894 86 Gratz, S. J. *et al.* Highly specific and efficient CRISPR/Cas9-catalyzed homology-directed repair in
895 Drosophila. *Genetics* **196**, 961-971, doi:10.1534/genetics.113.160713 (2014).
896 87 Port, F. & Bullock, S. L. Augmenting CRISPR applications in Drosophila with tRNA-flanked sgRNAs.
897 *Nat Methods* **13**, 852-854, doi:10.1038/nmeth.3972 (2016).
898 88 Bosch, J. A., Tran, N. H. & Hariharan, I. K. CoinFLP: a system for efficient mosaic screening and
899 for visualizing clonal boundaries in Drosophila. *Development* **142**, 597-606,
900 doi:10.1242/dev.114603 (2015).
901 89 Long, X., Colonell, J., Wong, A. M., Singer, R. H. & Lionnet, T. Quantitative mRNA imaging
902 throughout the entire Drosophila brain. *Nat Methods* **14**, 703-706, doi:10.1038/nmeth.4309
903 (2017).
904 90 Marshall, O. J., Southall, T. D., Cheetham, S. W. & Brand, A. H. Cell-type-specific profiling of
905 protein-DNA interactions without cell isolation using targeted DamID with next-generation
906 sequencing. *Nat Protoc* **11**, 1586-1598, doi:10.1038/nprot.2016.084 (2016).
907 91 Marshall, O. J. & Brand, A. H. damidseq_pipeline: an automated pipeline for processing DamID
908 sequencing datasets. *Bioinformatics* **31**, 3371-3373, doi:10.1093/bioinformatics/btv386 (2015).
909 92 Hulsen, T., de Vlieg, J. & Alkema, W. BioVenn - a web application for the comparison and
910 visualization of biological lists using area-proportional Venn diagrams. *BMC Genomics* **9**, 488,
911 doi:10.1186/1471-2164-9-488 (2008).
912 93 Huang da, W., Sherman, B. T. & Lempicki, R. A. Systematic and integrative analysis of large gene
913 lists using DAVID bioinformatics resources. *Nat Protoc* **4**, 44-57, doi:10.1038/nprot.2008.211
914 (2009).
915 94 Huang da, W., Sherman, B. T. & Lempicki, R. A. Bioinformatics enrichment tools: paths toward
916 the comprehensive functional analysis of large gene lists. *Nucleic Acids Res* **37**, 1-13,
917 doi:10.1093/nar/gkn923 (2009).
918 95 Robinson, J. T. *et al.* Integrative genomics viewer. *Nat Biotechnol* **29**, 24-26,
919 doi:10.1038/nbt.1754 (2011).
920 96 Schindelin, J. *et al.* Fiji: an open-source platform for biological-image analysis. *Nat Methods* **9**,
921 676-682, doi:10.1038/nmeth.2019 (2012).

922

Figure 1

A

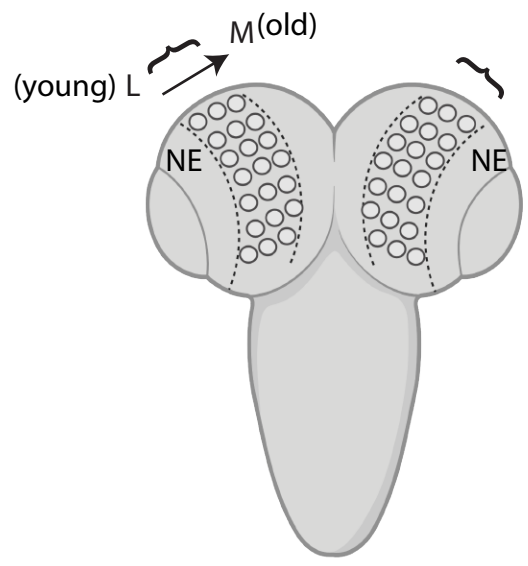
Medulla neuroblasts
M (old)
(young) L
NE
NE

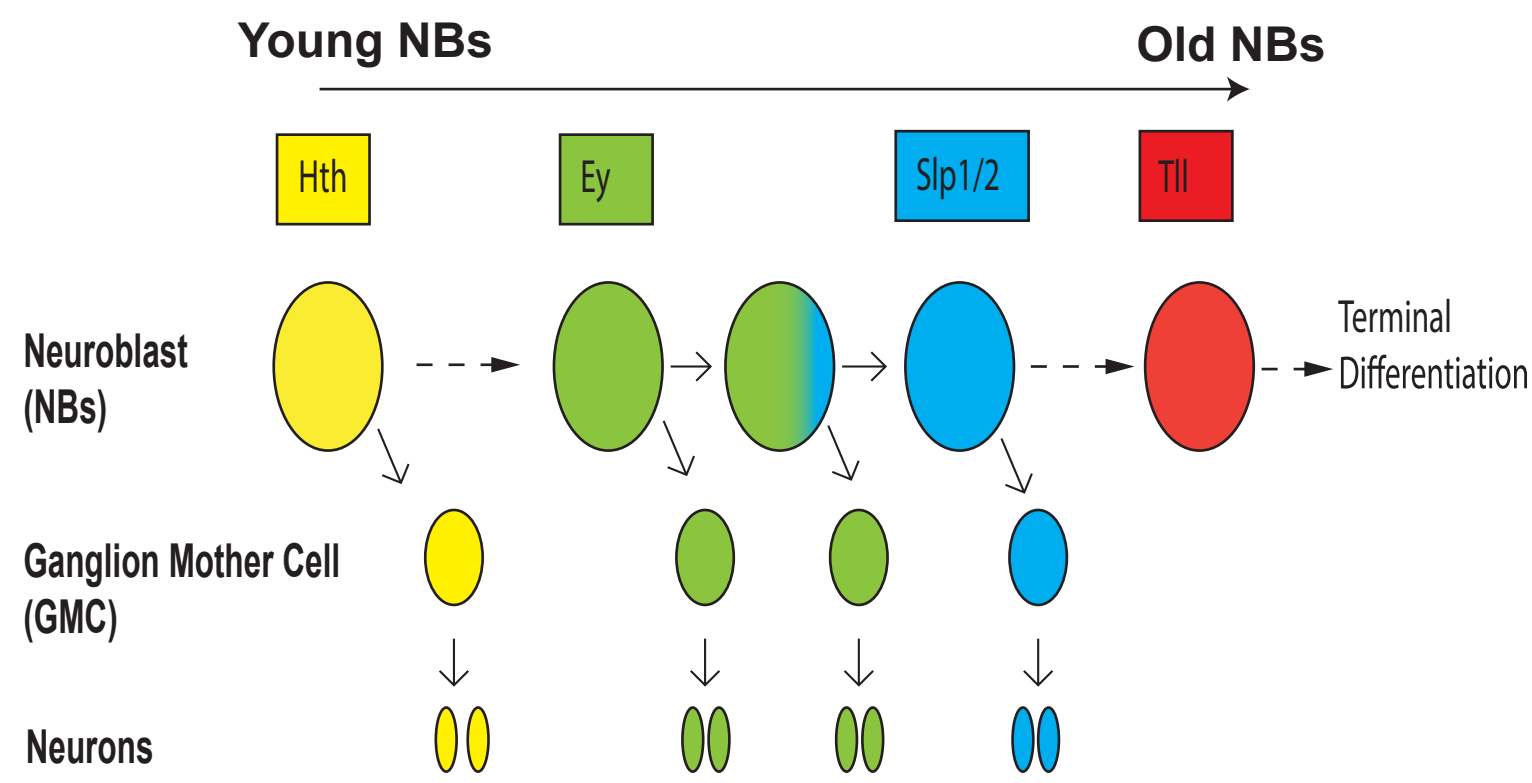
Young NBs
Old NBs
Hth
Ey
Slp1/2
Tll
Neuroblast (NBs)
Terminal Differentiation
Ganglion Mother Cell (GMC)
Neurons

D

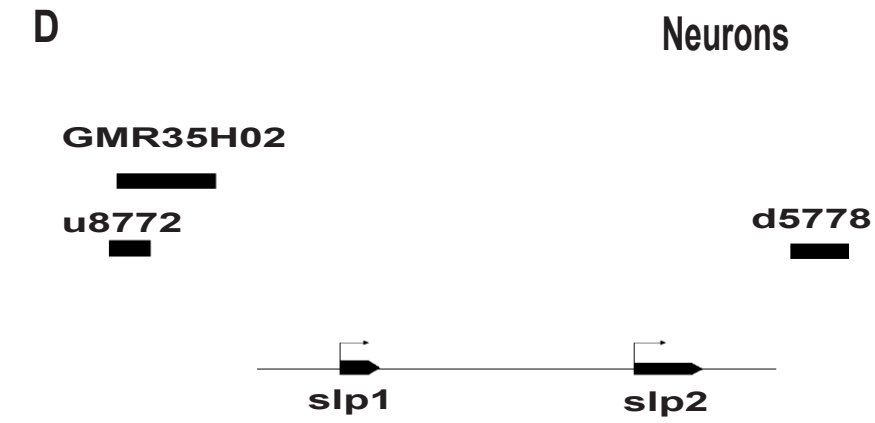
GMR35H02
u8772
d5778
slp1
slp2

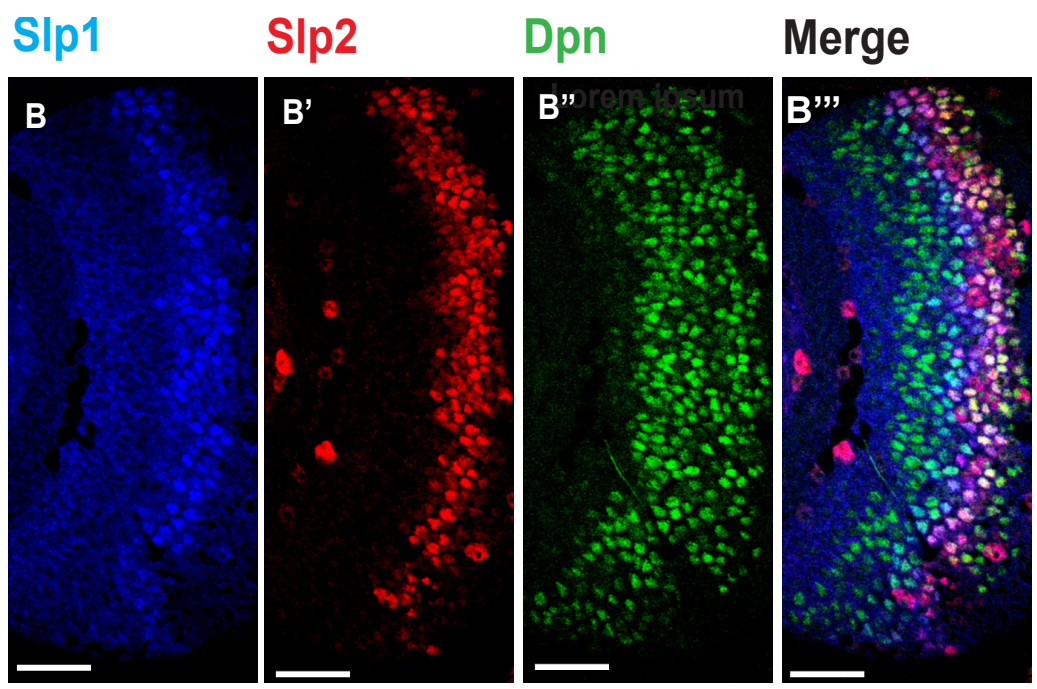
Slp1
Slp2
Dpn
Merge
B
B'
B''
B'''

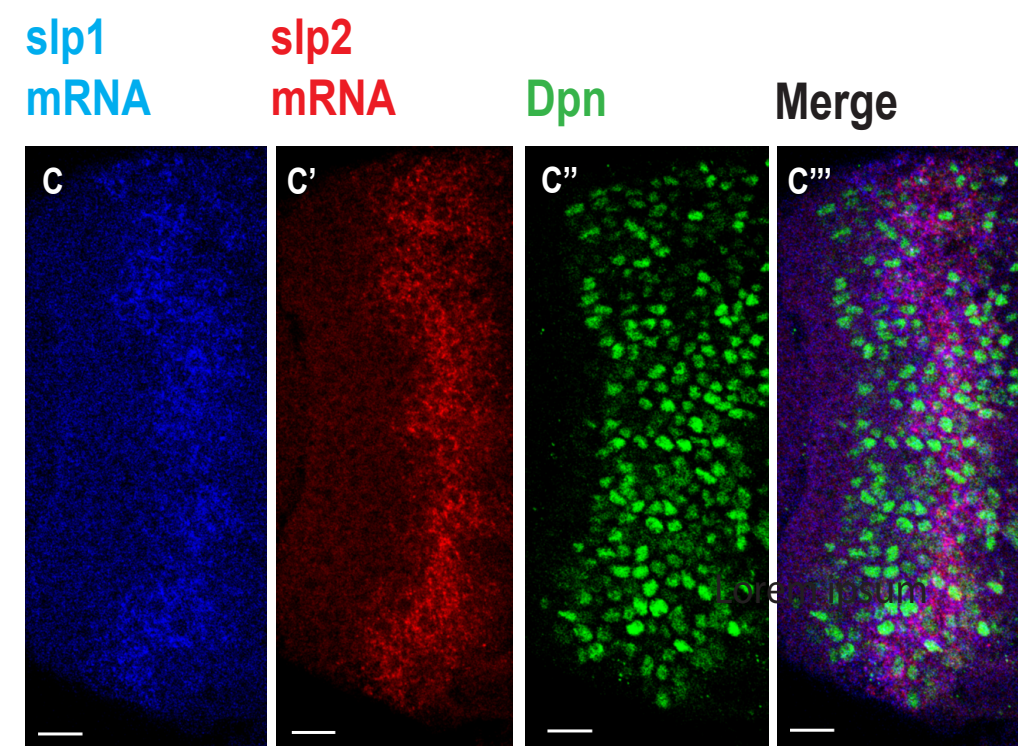
slp1 mRNA
slp2 mRNA
Dpn
Merge
C
C'
C''
C'''

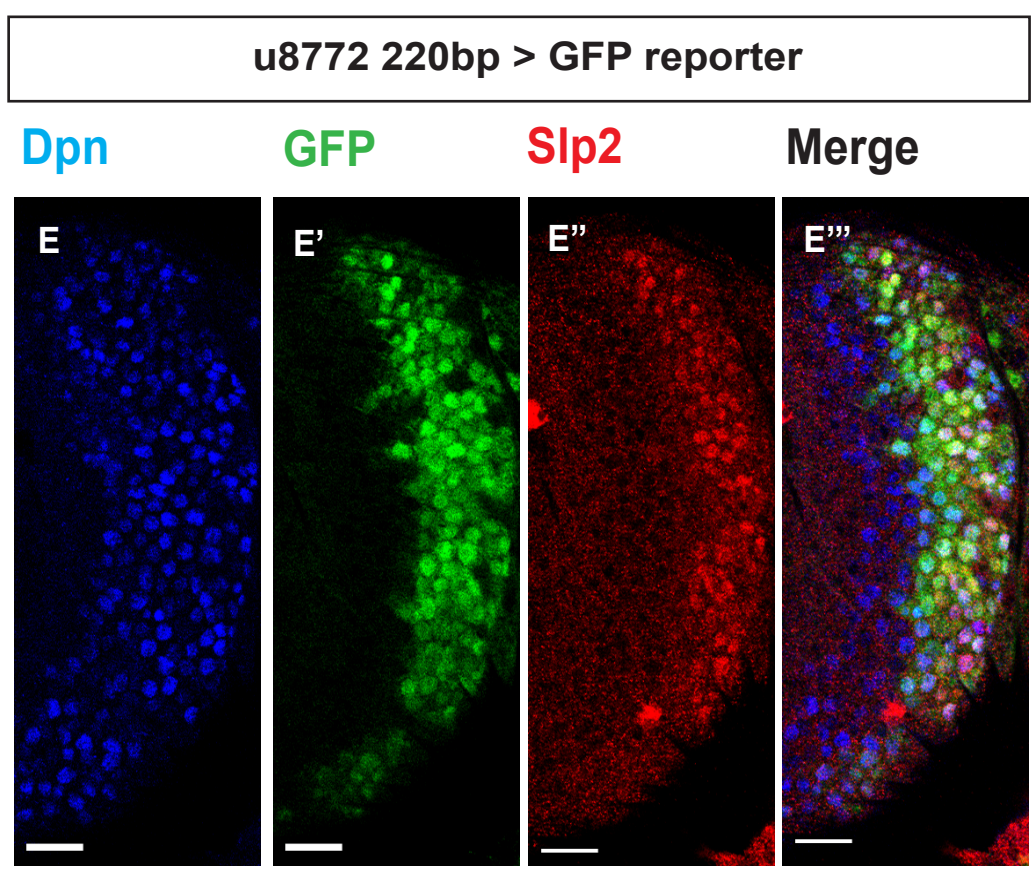
u8772 220bp > GFP reporter
Dpn
GFP
Slp2
Merge
E
E'
E''
E'''

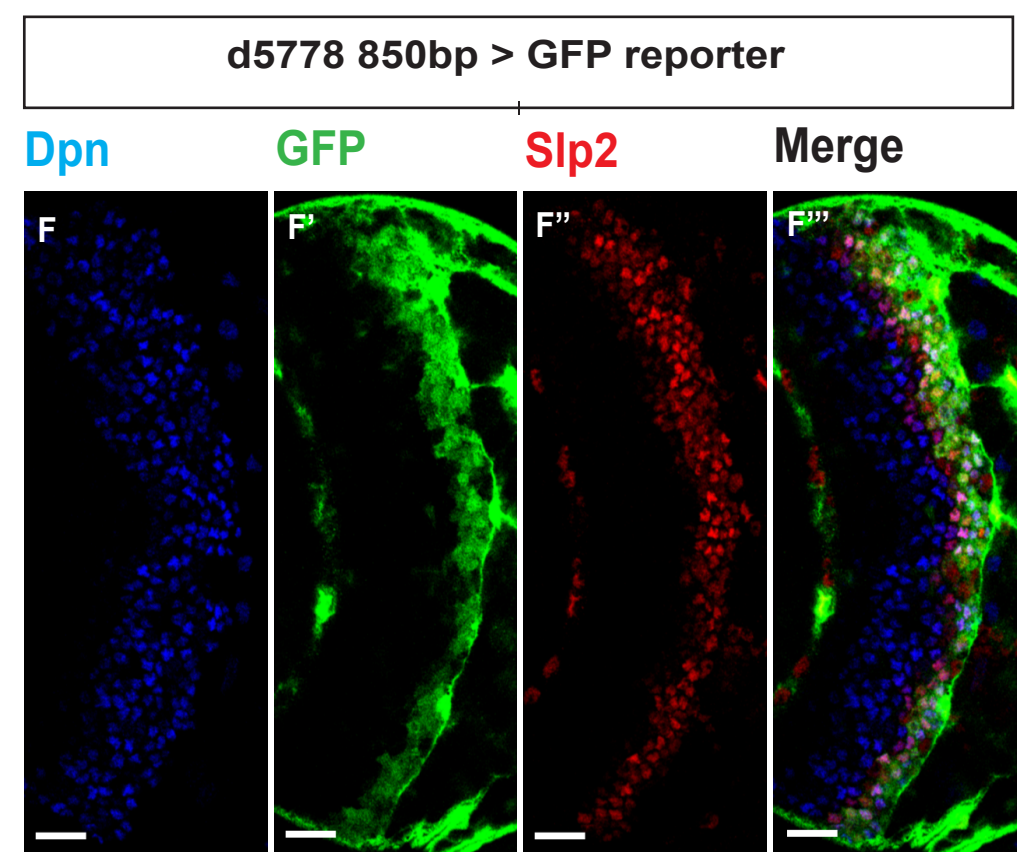
d5778 850bp > GFP reporter
Dpn
GFP
Slp2
Merge
F
F'
F''
F'''

Figure 1. Expression of *slp1* and *slp2* genes in medulla neuroblasts is controlled at transcription and achieved by coordinated action of at least two transcriptional enhancers. (A) Schematic of *Drosophila* brain at the third instar larval stage highlighting the location of the optic lobe medulla. Medulla NBs (shown as circles), located on the surface of the optic lobe, are transformed from neuroepithelial cells (NE) as a neurogenesis wave spreads in a medial to lateral direction. As a result, medulla NBs of different ages are aligned on the lateral (L) to medial (M) spatial axis. Schematic to the right shows part of the temporal patterning program of medulla NBs with a focus on the Ey to Slp1/2 transition. NBs undergo asymmetric divisions to self-renew and to produce intermediate progenitors called Ganglion Mother Cells that each divide once to produce two neurons. In the Ey stage, NBs undergo a few divisions while gradually turning on Slp expression, thus there is a significant overlap between Ey and Slp expression in NBs. After Slp level reaches a certain threshold, the transition occurs. Several such transitions later as indicated by the dashed arrow neuroblasts express TTF Tailless before entering the final stage to undergo terminal differentiation. The larval brain graphic was created using BioRender. (B) Expression patterns of Slp1 and Slp2 proteins in medulla neuroblasts identified by their expression of Deadpan (Dpn, a neuroblast marker). (C) Expression patterns of Slp1 and Slp2 mRNAs in Dpn expressing medulla neuroblast closely parallels the corresponding protein expression patterns. (D) Schematic of the relative locations of *slp1* and *slp2* genes and transcriptional enhancers identified as regulating their expression. Positions of slp1 coding locus (2L:3,825,675..3,827,099 [+]), slp2 coding locus (2L:3,836,840..3,839,185 [+]), GMR35H02 (2L:3,817,265..3,821,014) and the REDfly enhancers u8772 (2L:3,816,967..3,818,532) and d5778 (2L:3,842,530..3,844,660) are shown relative to one another. A 220 bp enhancer located within the genomic segment covered by GMR35H02 and an 850 base pair enhancer element within the REDFly enhancer d5778 were identified as potential cis-regulatory elements of *slp1* and *slp2* genes. The distance between the start of GMR35H02 and the end of d5778 is around 27.394 kbp. (E) Expression patterns of a GFP reporter expressing GFP driven by the 220 bp enhancer closely approximates endogenous expressions of Slp1 and Slp2 in medulla neuroblasts. (F) Expression pattern of GFP reporter driven by the 850 bp enhancer shown alongside endogenous Slp1/2 expressions. This enhancer initiates GFP expression at a slightly later stage compared to the 220 bp enhancer and likely also regulates Slp2 expression in surface glia. Scale bar: 20 microns.

Figure 2

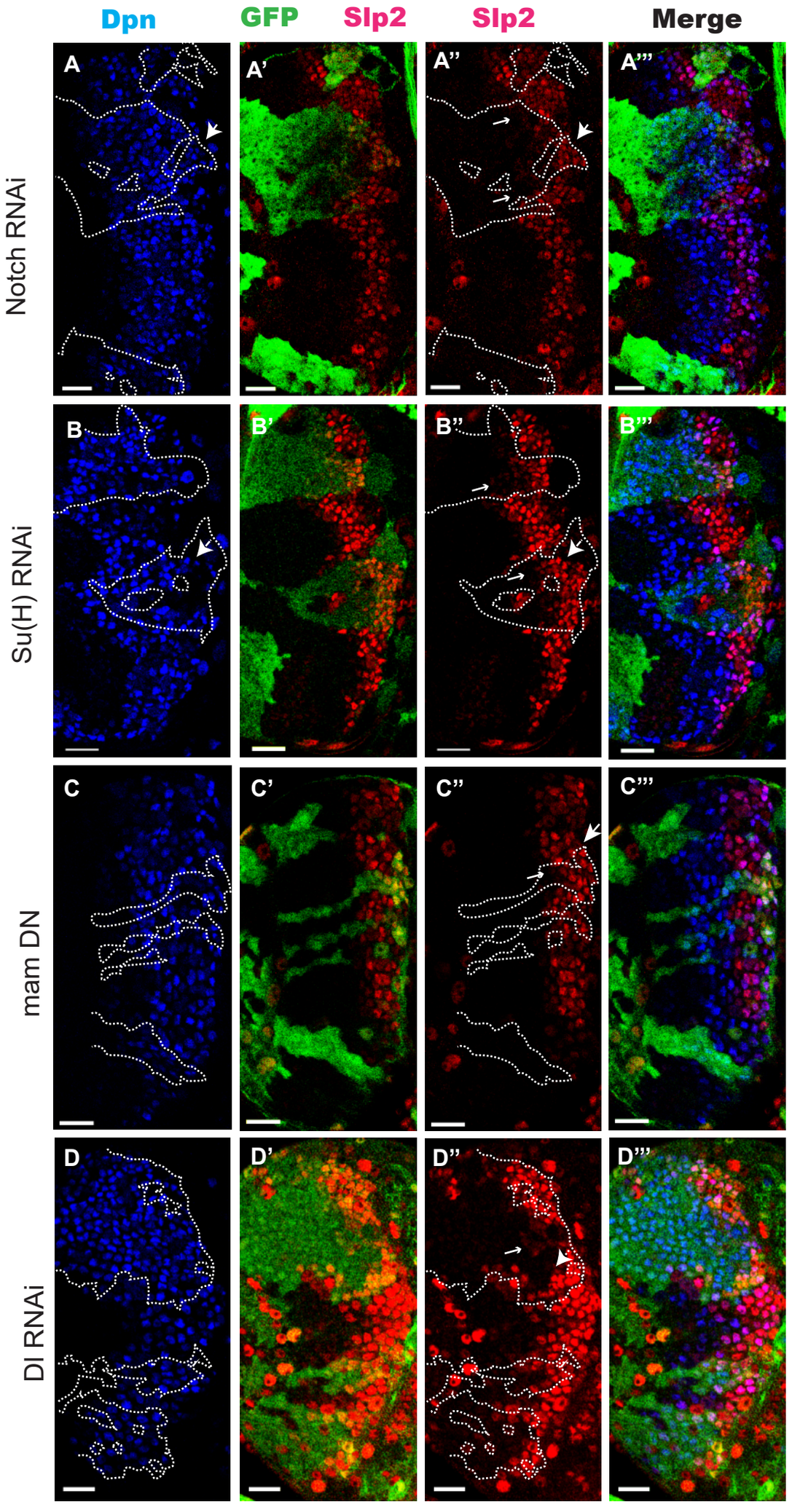
Dpn
GFP
Slp2
Slp2
Merge
Notch RNAi
Su(H) RNAi
mam DN
Dl RNAi
A
A'
A''
A'''
B
B'
B''
B'''
C
C'
C''
C'''
D
D'
D''
D'''

Figure 2. The Notch pathway regulates expression of *slp* genes in medulla neuroblasts. (A) RNAi knockdown of Notch in GFP marked clones leads to a delay in expression of Slp2 compared to contemporaneous wild type neuroblasts outside the GFP marked clones. (B) RNAi knockdown of Su(H) shows a similar delay in Slp2 expression as for Notch-RNAi. (C) Expression of a dominant negative variant of Mastermind, third component of the Notch transcription complex shows a similar phenotype as *N RNAi* and *Su(H) RNAi* and delays Slp2 expression. (D) Knockdown of Dl, a Notch ligand, caused a similar delay in Slp2 expression. All clones are generated with *ayGal4 UAS GFP* and clone boundaries are shown in dotted lines. Arrows indicate that Slp2 expression is delayed in the clones. Scale bar 20 microns.

Figure 3

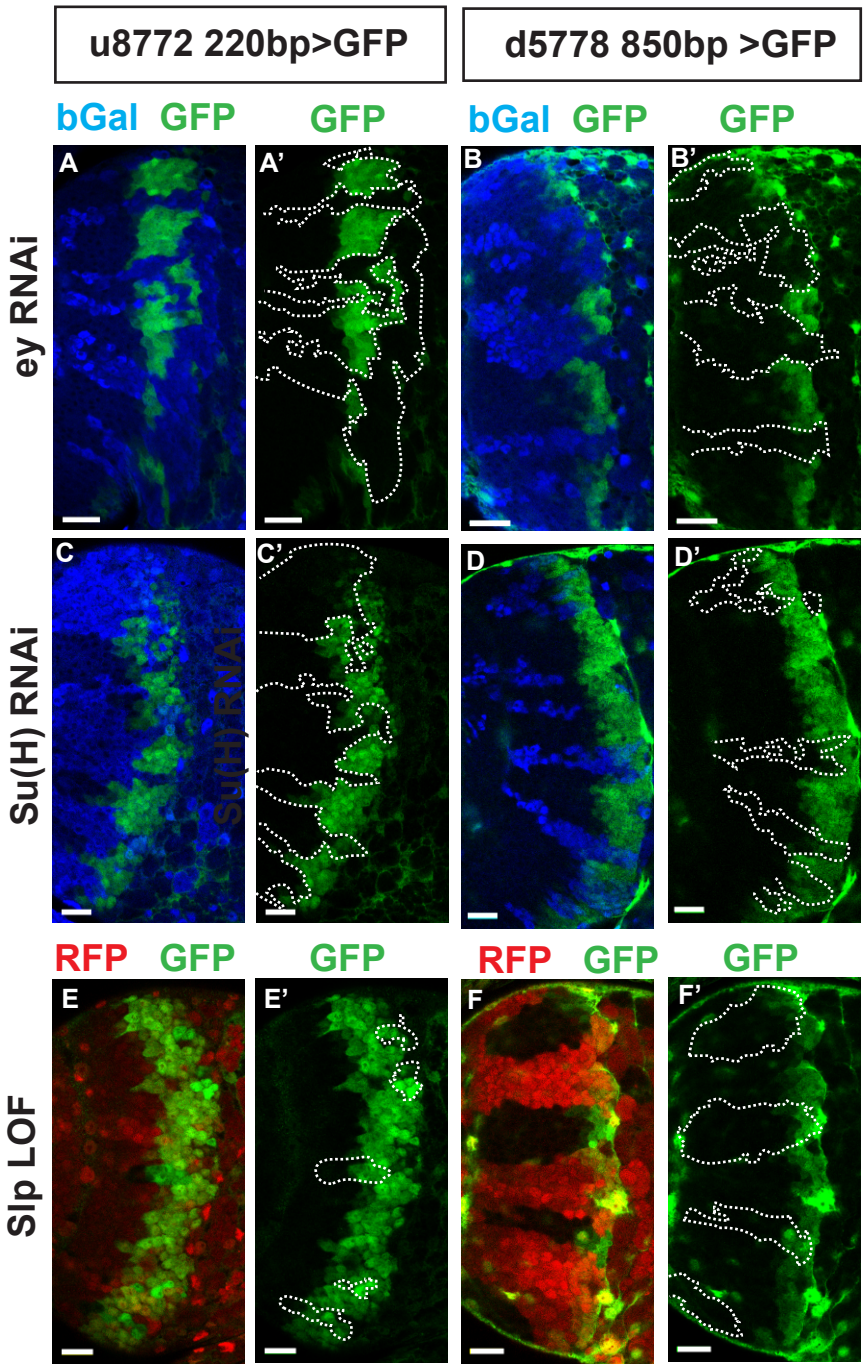
u8772 220bp>GFP
d5778 850bp >GFP
bGal GFP
GFP
bGal GFP
GFP
ey RNAi
A
A'
B
B'
Su(H) RNAi
C
C'
D
D'
RFP GFP
GFP
RFP GFP
GFP
Slp LOF
E
E'
F
F'

Figure 3. Eyeless and the Notch pathway act through the 220 bp and 850 bp enhancers to regulate expression of *slp* genes. (A-D') RNAi clones in which Ey or Su(H) is knocked down are marked by *Beta-galactosidase* (*bGal*) in blue, while regions unmarked by *bGal* are populated by wild type neuroblasts. (A,A') Observed expression of a GFP reporter driven by the 220 bp enhancer element in *Ey RNAi* clones and wild type neuroblasts. (B,B') Observed expression of a GFP reporter driven by the 850 bp enhancer element in *Ey RNAi* knockdown clones and in wild type neuroblasts. In case of both enhancers knockdown of Ey leads to a loss of GFP reporter expression. (C,C') The expression of the GFP reporter driven by 220bp enhancer in Su(H) RNAi clones and in wild type neuroblasts. (D,D') The expression of the GFP reporter driven by 850bp enhancer in Su(H) RNAi clones and in wild type neuroblasts. In case of both enhancers expression of the GFP reporter is lost or delayed. (E, E') Expression of the 220 bp GFP reporter in *slp1* and *slp2* loss of function mitotic clones ('dark' regions) and in wild type neuroblasts (marked by RFP). (F,F') Expression of the 850 bp enhancer GFP reporter in *slp* LOF clones and wild type neuroblasts similar to (E,E'). Slp1 binding sites were identified in both enhancer elements which indicate that Slp may auto-regulate their expression. However, GFP reporter expression driven by these two enhancers is not significantly affected within *slp* LOF neuroblasts, suggesting that Slp1/2 are not required to initiate their own expression in neuroblasts. Scale bar 20 microns.

Figure 4

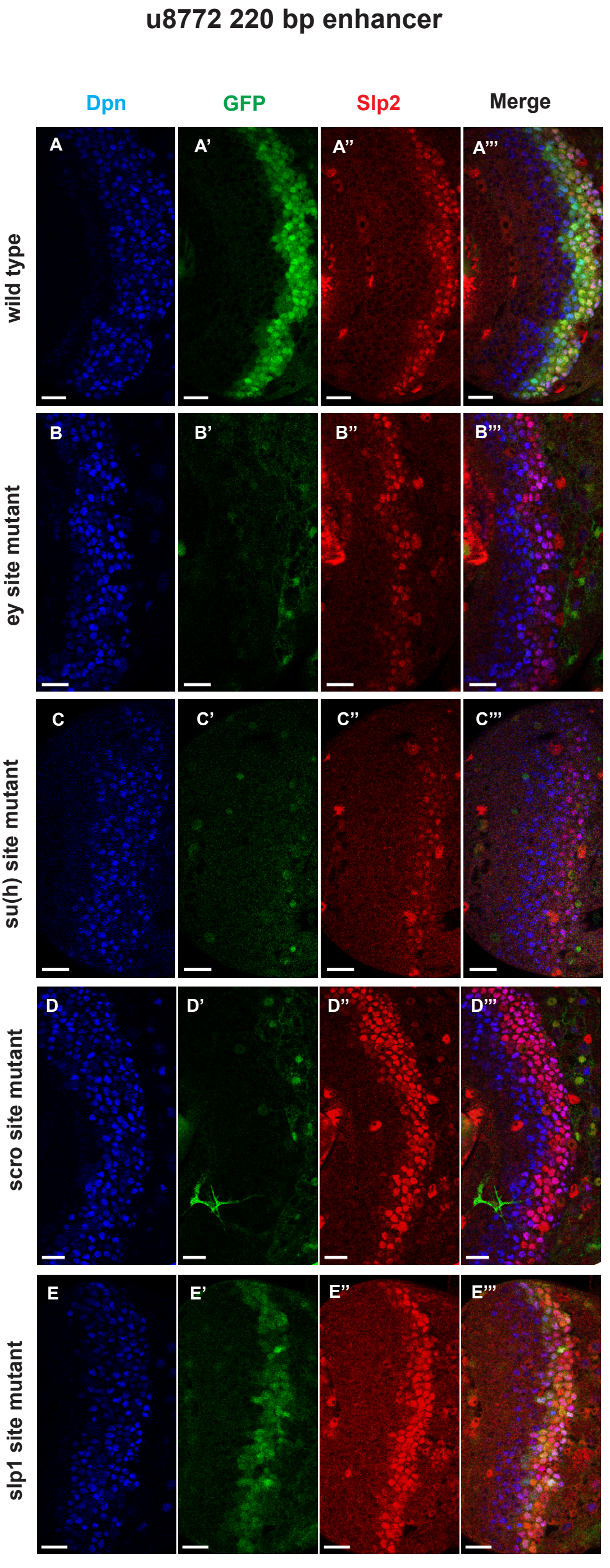
u8772 220 bp enhancer
Dpn
GFP
Slp2
Merge
wild type
ey site mutant
su(h) site mutant
scro site mutant
slp1 site mutant
A
A'
A''
A'''
B
B'
B''
B'''
C
C'
C''
C'''
D
D'
D''
D'''
E
E'
E''
E'''

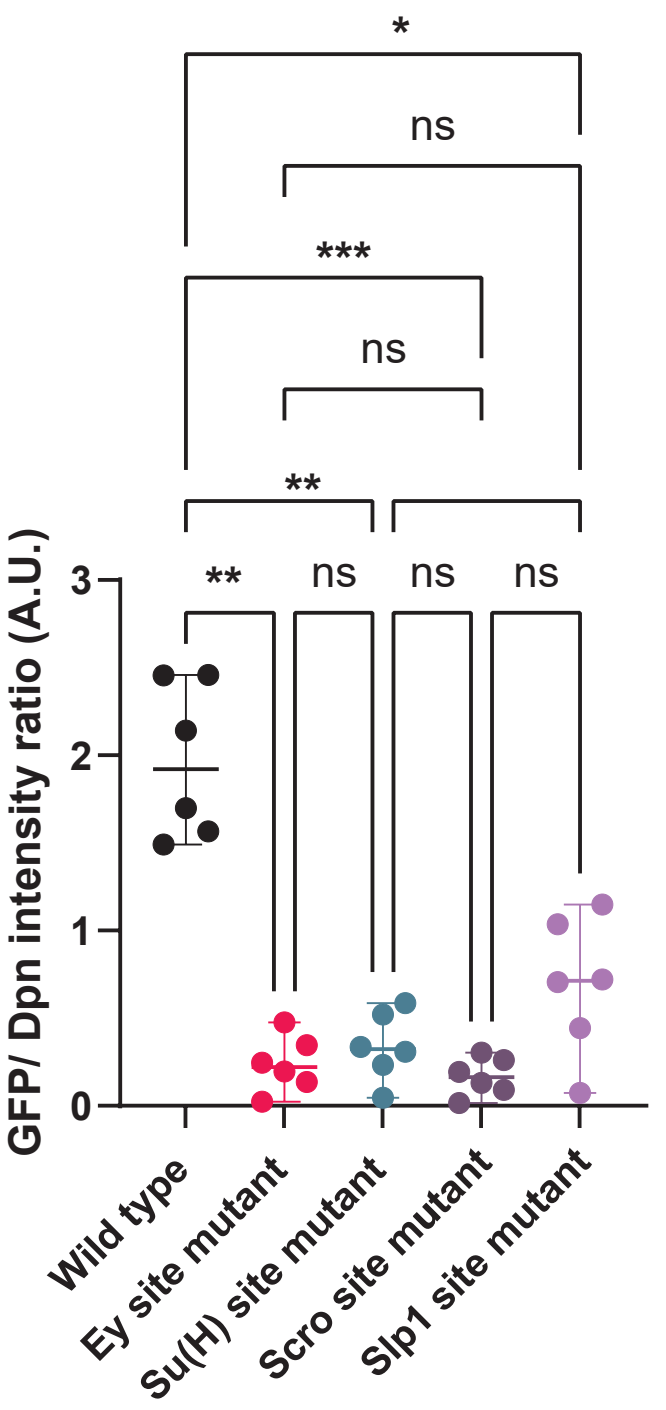
F
u8772 220bp GFP reporters
GFP/ Dpn intensity ratio (A.U.)
0
1
2
3
*
ns
***
ns
**
**
ns
ns
ns
Wild type
Ey site mutant
Su(H) site mutant
Scro site mutant
Slp1 site mutant

Figure 4. Mutations of putative binding sites for Ey, Su(H) and Scro in u8772 220 bp enhancer confirm their requirement for activating expression of Slp1/2 genes. Expression of GFP reporter driven by the wild-type 220 bp enhancer (A-A’’’) was compared against GFP reporters driven by mutated versions of the 220 bp enhancer in which predicted binding sites for specific transcription factors had been mutated: (B-B’’’) with predicted Ey binding sites mutated, (C-C’’’) with predicted Su(H) binding sites mutated, (D-D’’) with predicted Scro binding sites mutated, (E-E’’’) Slp1 binding sites mutated. Loss of binding sites for Ey, Su(H) and Scro in the 220 bp enhancer led to a loss of GFP reporter expression. Scale bar: 20 microns. F. Intensity comparisons of mutated and wild type GFP reporters of the u8772 220bp enhancer. The decrease in intensity of GFP expression for Ey , Scro, Su(H) and Slp1 binding site mutated reporters relative to wild type are all statistically significant (RM One-way ANOVA was performed with the Geisser-Greenhouse correction, p value 0.0001; this was statistically significant, since $p < 0.05$. Adjusted p values from Tukey’s multiple comparison test for mutants versus wild type are as follows: for Ey mutant $p = 0.0013$, for Su(H) mutant $p = 0.0032$, for Scro site mutant $p = 0.0007$, for Slp1 site mutant $p = 0.0225$. Six different sets of observations were used for quantification (n=6)). Graphs indicate mean and 95% C.I. and distributions of each data point about the mean.

Figure 5

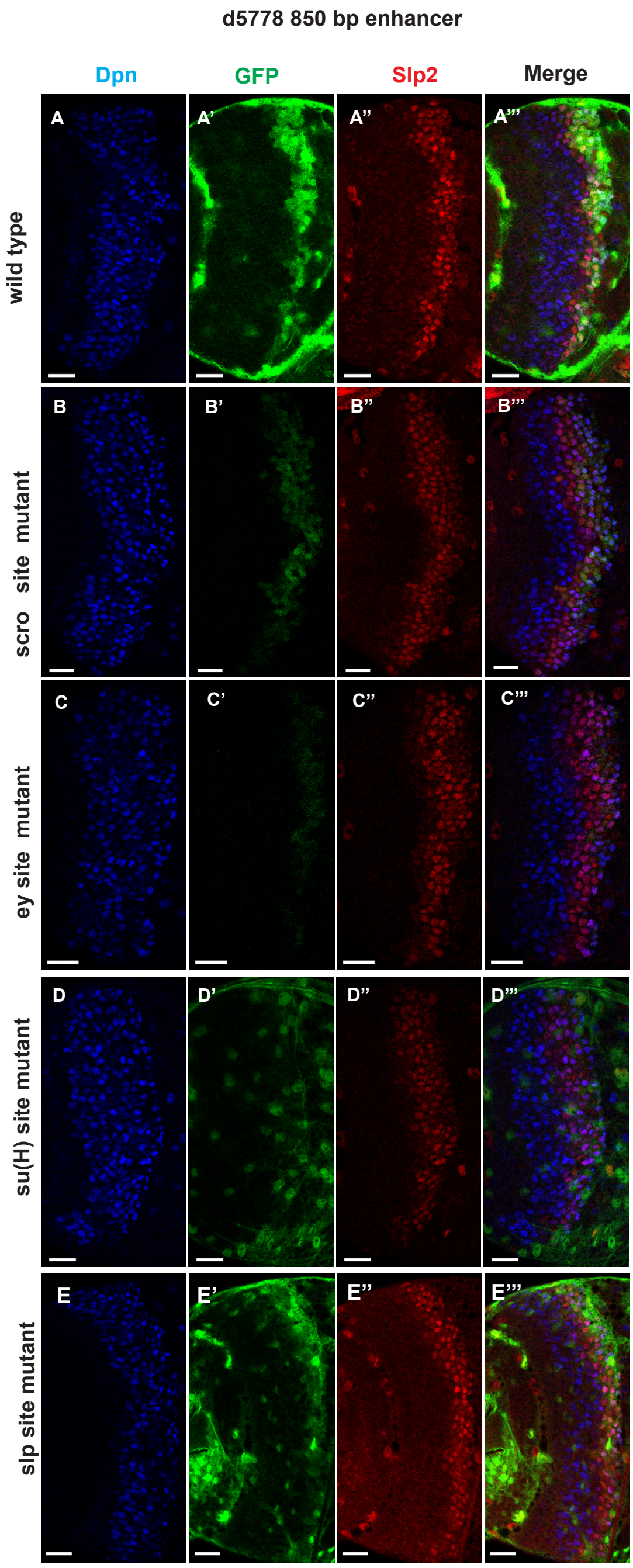

F. A comparison of d5778 850bp reporters

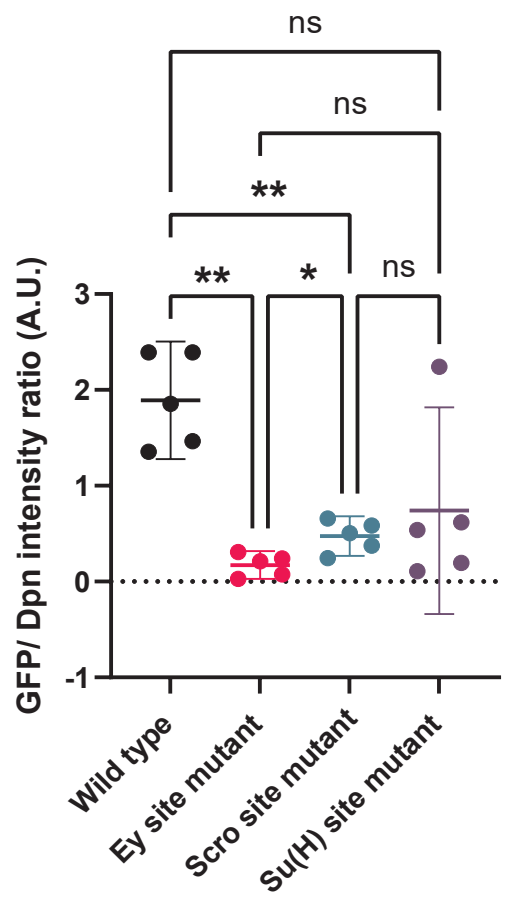

Figure 5. Mutations of putative binding sites for Ey, Su(H) and Scro in d5778 850 bp enhancer confirm their requirement for activating expressions of Slp1/2 genes. A parallel comparison was made for GFP reporter expression driven by the wild type 850 bp enhancer (A-A’’’) to the GFP reporter expression driven by versions of the 850 bp enhancer with binding sites for specific transcription factors Scro, Ey, Su(H) and Slp1 mutated (B-B’’’, C-C’’’, D-D’’’, and E-E’’’ respectively). Loss of binding sites for Ey nearly obliterated GFP reporter expression in neuroblasts as did the loss of Su(H) binding sites. Additionally, in Su(H) site mutant expression of GFP reporter was up-regulated in surface glial cells. Loss of potential Scro binding sites also greatly reduced GFP reporter expression. Loss of Slp1 binding sites did not lead to a significant reduction in intensity (E-E’’’). Scale bars: 20 microns. (F) Quantitation of d5778 850bp reporter intensities of the wild type and the factor binding site mutated variants shows that the reduction of GFP intensity compared to wild type for Ey binding site and Scro binding site mutated reporters is statistically significant (RM one-way ANOVA was performed with the Geisser-Greenhouse correction and p value was calculated to be 0.005; this was statistically significant as $p < 0.05$. Adjusted p values from Tukey’s multiple comparison test between wild type and mutants are as follows: for Ey site mutant $p = 0.0027$, for Scro site mutant $p = 0.0087$, for Su(H) site mutant $p = 0.1076$. Five different sets of observations were used for quantification ($n=5$)). For the Su(H) site mutated variant, though GFP expression was visibly reduced in neuroblasts, the unavoidable contributions of GFP signals from surface glial cells has confounded our measurements of GFP reporter intensity, making GFP signals appear stronger and the intensity reduction relative to wild type statistically insignificant.

Figure 6

A.

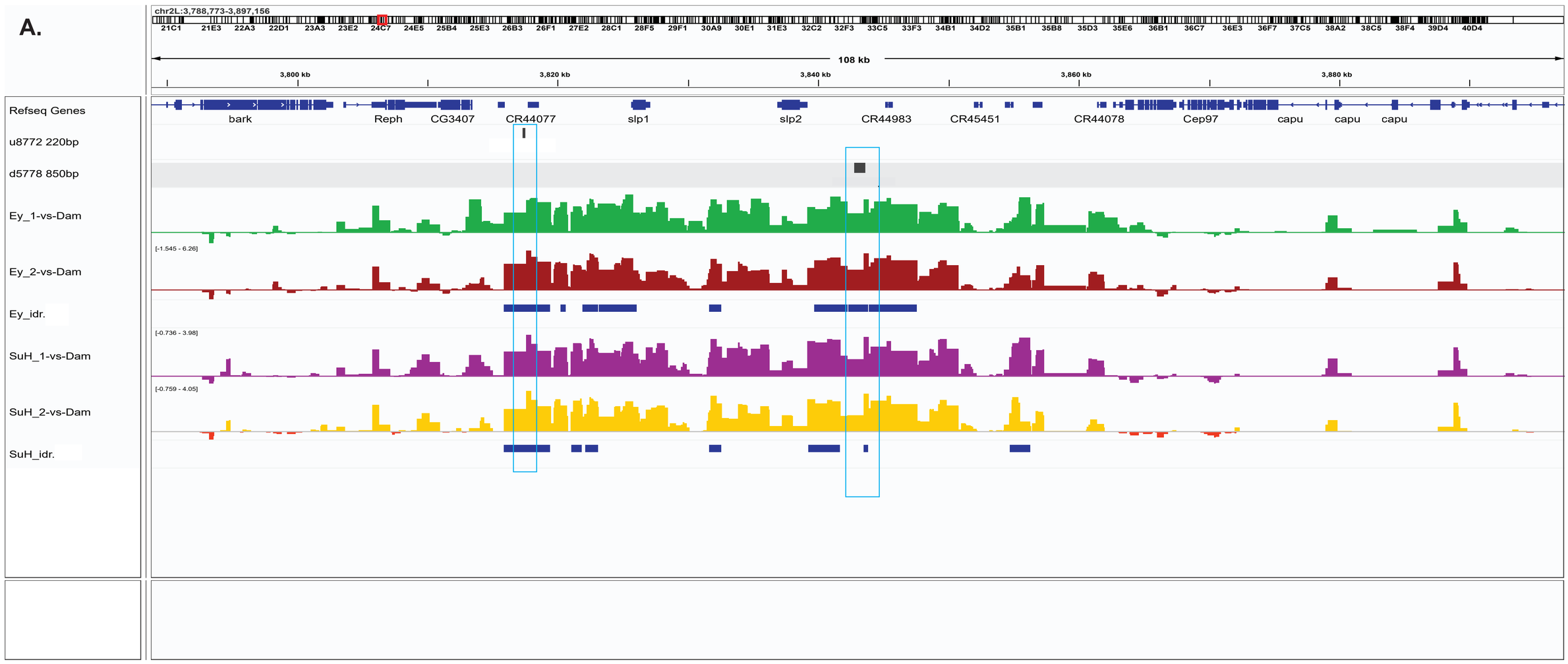

C.GO Term: Asymmetric Cell Division

CG3779-RB(numb)
G protein alpha i subunit(Galphai)
Notch(N)
brain tumor(brat)
frizzled(fz)
neuralized(neur)
prospero(pros)

D. GO Term: Cell division

Cyclin A(CycA)
Cyclin E(CycE)
Cyclin G(CycG)
diaphanous(dia)
peanut(pnut)
pontin(pont)
string(stg)

E. GO Term:Apical Cell Polarity

Abl tyrosine kinase(Abl)
CG42684 gene product from transcript CG42684-RB
G protein alpha i subunit(Galphai)
TNF-receptor-associated factor 4 (Traf4)
brain tumor(brat)
miranda(mira)
prospero(pros)

F. GO Term: Nuclear hormone receptor

Ecdysone receptor(EcR)
Ecdysone-induced protein 75B (Eip75B)
knirps-like(knrl)

B. Overlap between Ey-Dam and Su(H)-Dam bound genes

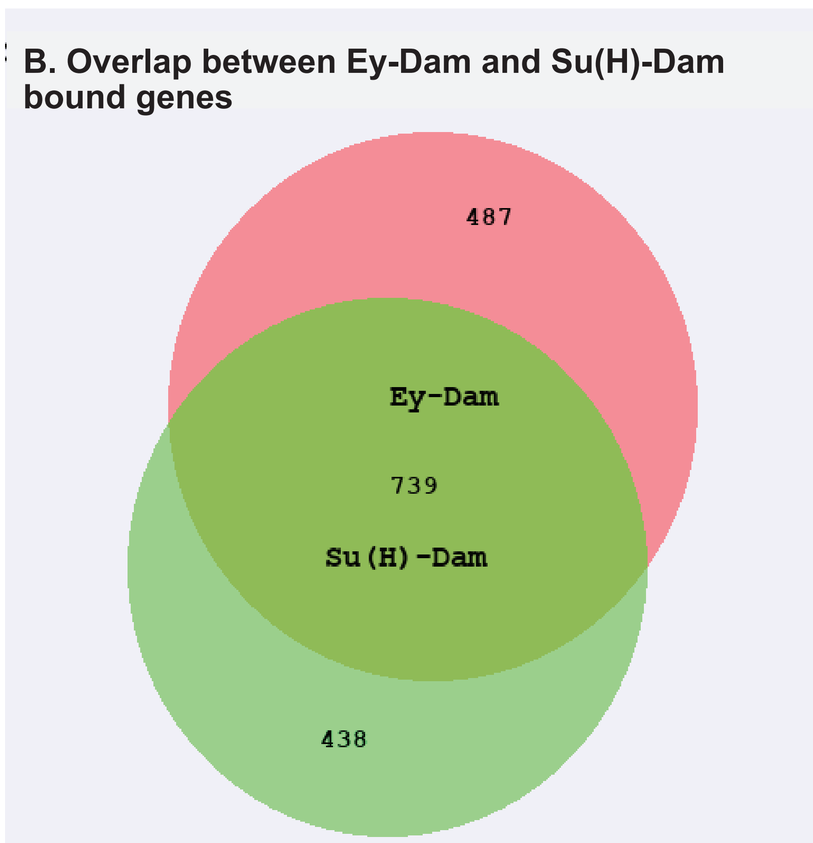

G. GO Term:Notch

Abl tyrosine kinase(Abl)
Beadex(Bx)
Bearded(Brd)
numb
E(spl)m8-HLH
E(spl)mbeta-HLH
E(spl)mdelta-HLH
E(spl)mgamma-HLH
Epidermal growth factor receptor
Neurotactin(Nrt)
Serrate(Ser)
Star(S)
atonal(ato)
big brain(bib)
canoe(cno)
enabled(ena)
extra macrochaetae(emc)
fringe(fng)
frizzled(fz)
longitudinals lacking(lola)
neuralized(neur)
patched(ptc)
plexus(px)
pointed(pnt)
polychaetoid(pyd)
prickle(pk)
string(stg)
tribbles(trbl)

H. GO Term: Axon guidance

Abl tyrosine kinase(Abl)
CG14662
Sema-1a
Unc-115a
comm2
unc-5
jing
Cadherin-N(CadN)
Dscam1
GUK-holder(gukh)
Insulin-like receptor(InR)
Neurotactin(Nrt)
Notch(N)
Protein tyrosine phosphatase 61F(Ptp61F)
Trim9
apterous(ap)
brain tumor(brat)
capricious(caps)
earmuff(erm)
enabled(ena)
eyes absent(eya)
frazzled(fra)
frizzled 2(fz2)
longitudinals lacking(lola)
misshapen(msn)
multiple edematous wings(mew)
nervous fingers 1(nerfin-1)
patched(ptc)
pou domain motif 3(pdm3)
prospero(pros)
roundabout 2(robo2)
scribbler(sbb)
single-minded(sim)
slit(sli)
tailup(tup)
target of Poxn(tap)
unzipped(uzip)

Figure 6. Genome-wide binding of Ey and Su(H) were examined by DamID-seq. (A) Prominent peaks of Ey and Su(H) binding are seen in neighborhood of the *slp1* and *slp2* gene loci including at the genomic locations of identified 220bp and 850 bp enhancers in both replicates of Ey-Dam and Su(H)-Dam experiments. Peaks at the u8772 220bp and the d5778 850bp enhancers have passed IDR< 0.05 cut-off supporting their reproducibility. (B) Output from BioVenn showing overlap between genes bound by EyDam and Su(H)Dam suggesting that Ey may act as a priming factor in recruiting Su(H) to enhancers of Notch-target genes in neuroblasts. (C-H) GO terms associated with genes that are bound by both Ey and Su(H) and thus may be co-regulated by Ey and the Notch pathway. Genes involved in a variety of processes relevant to neuroblasts and neural differentiation are seen.

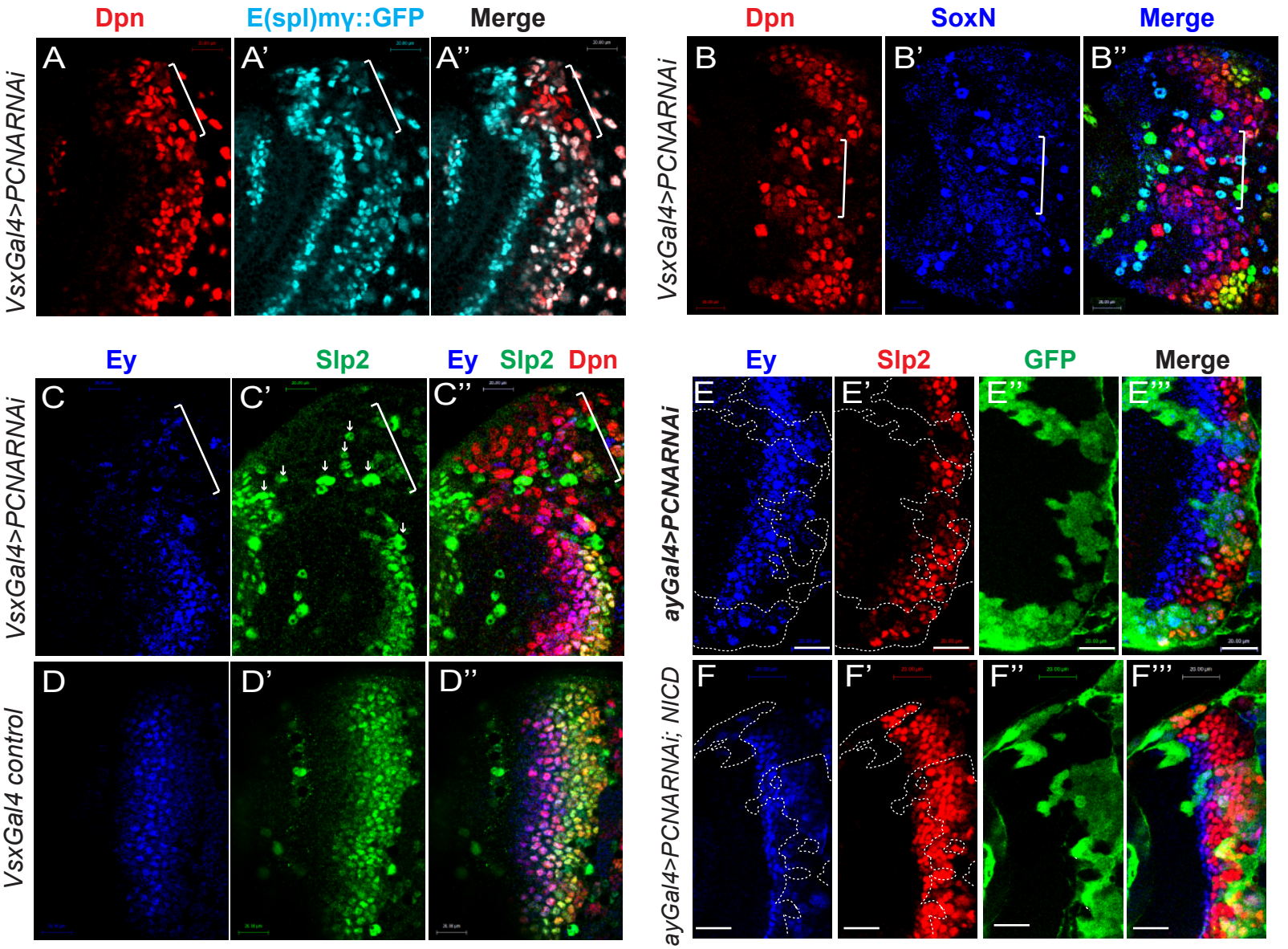

Figure 7. Cell cycle progression is required for the precise timing of Slp expression and this is mediated in part through Notch signaling.
(A-A'''') The expression of Dpn (red) and E(spl)mγGFP (cyan) in vsxGal4 driving UASDCR2 and UAS-PCNARNAi (VDRC51253) optic lobes (n=5). The affected domain is indicated by a bracket. (B-B'''') The expression of Dpn (red) and SoxN (blue) in vsxGal4 driving UASDCR2 and UAS-PCNARNAi optic lobes (n=5). (C-C'') The expression of Dpn (red), Ey (blue) and Slp2 (green) in vsxGal4 driving UASDCR2 and UAS-PCNARNAi optic lobes (n=9). The affected domain is indicated by a bracket. Some glia express Slp2 but not Dpn are indicated by white arrows. (D-D'') The expression of Dpn (red), Ey (blue) and Slp2 (green) in vsxGal4; UASDCR2 control optic lobes. (E-E'''') Larvae of genotype ywhsFLP; ayGal4UASGFP /UAS-PCNARNAi; UASDCR2/+ were heat shocked at 37C for 8min 70 hours before dissection at 3rd instar larval stage. Ey expression (blue) is minimally affected in clones marked by GFP (green), while Slp2 (red) expression is delayed (17 clones). (F-F'''') Larvae of genotype ywhsFLP; ayGal4UASGFP /UAS-PCNARNAi; UASDCR2/dpn>FRT-STOP-FRT-NICD were heat shocked at 37C for 8min 70 hours before dissection at 3rd instar larval stage. Ey expression (blue) is minimally affected in clones marked by GFP (green), while Slp2 (red) expression initiation is rescued (10 clones). Scale bar 20 microns.

Supplementary Figure S1

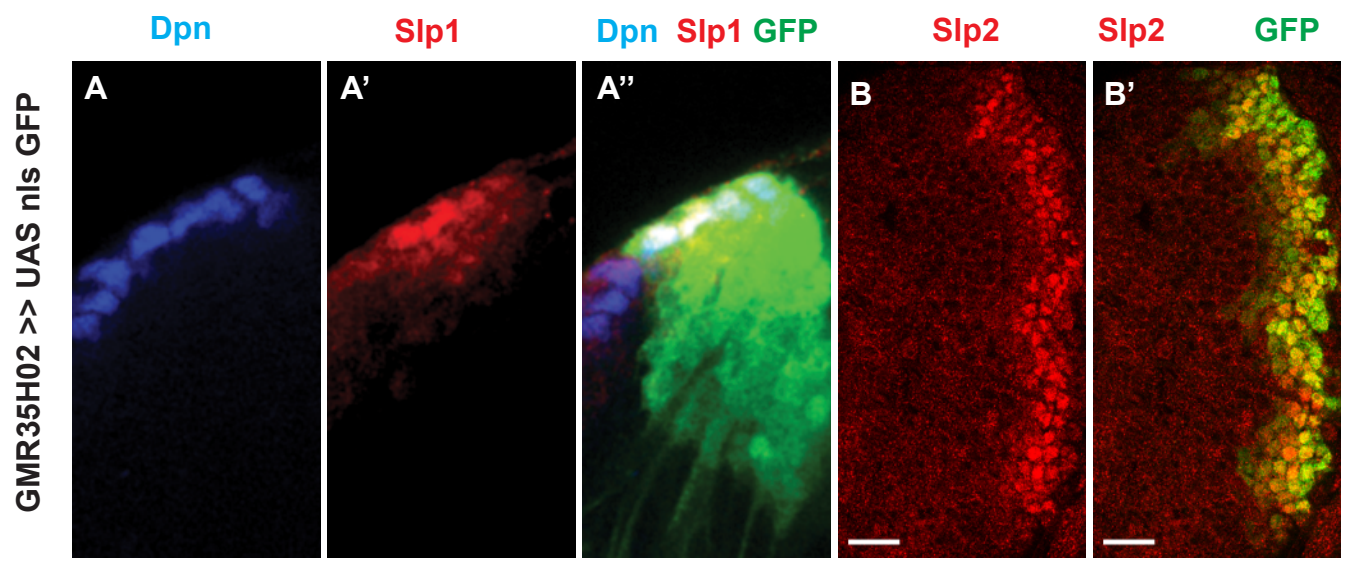

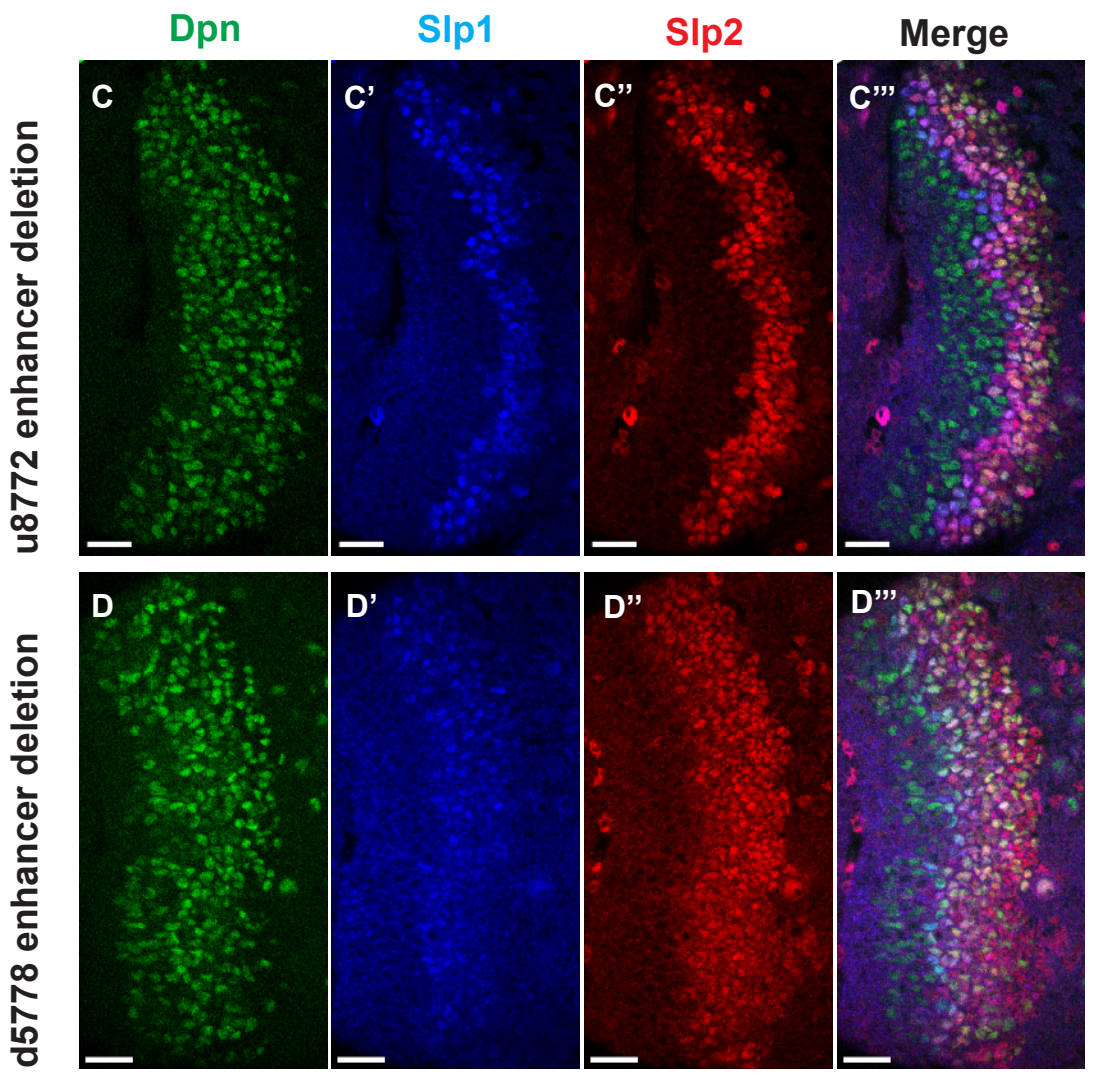

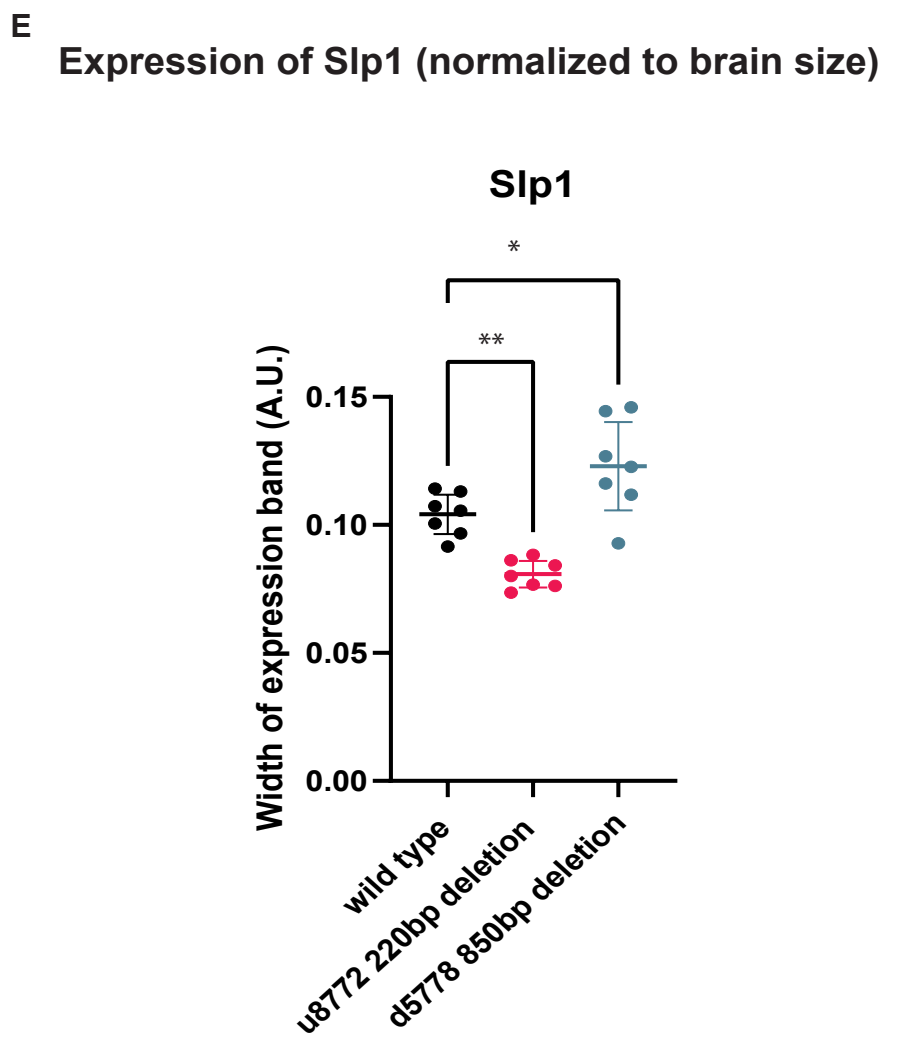

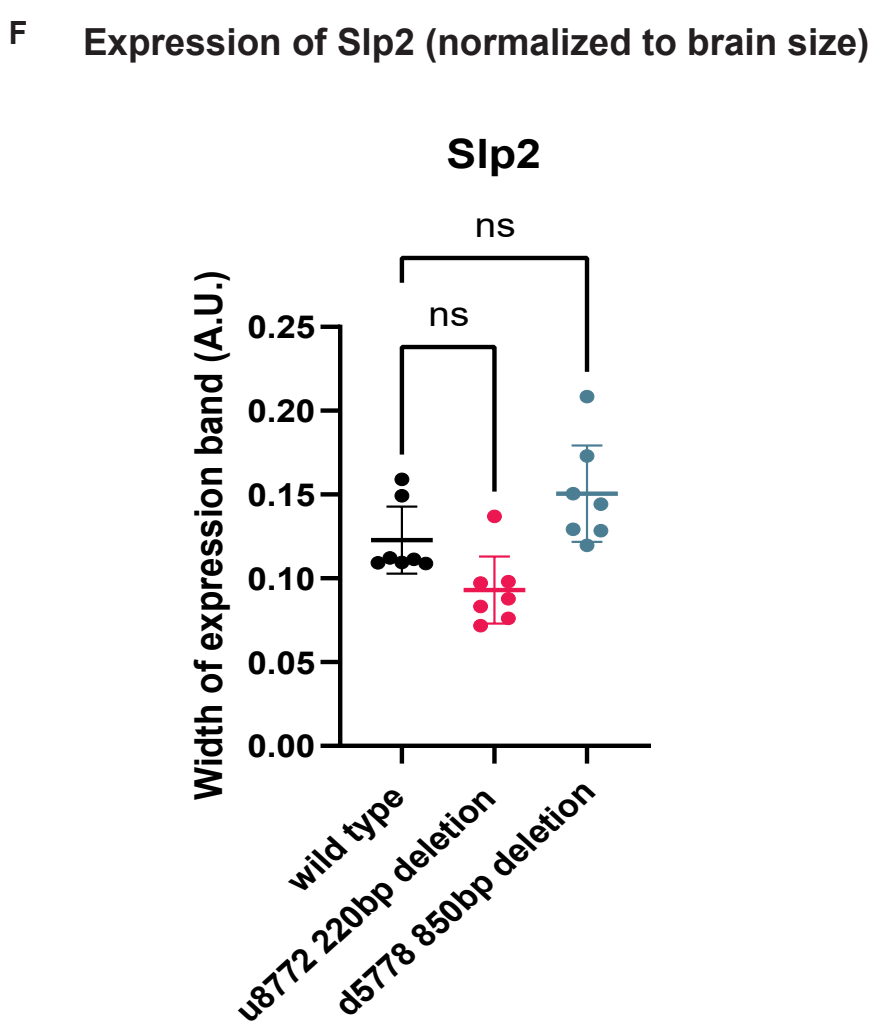

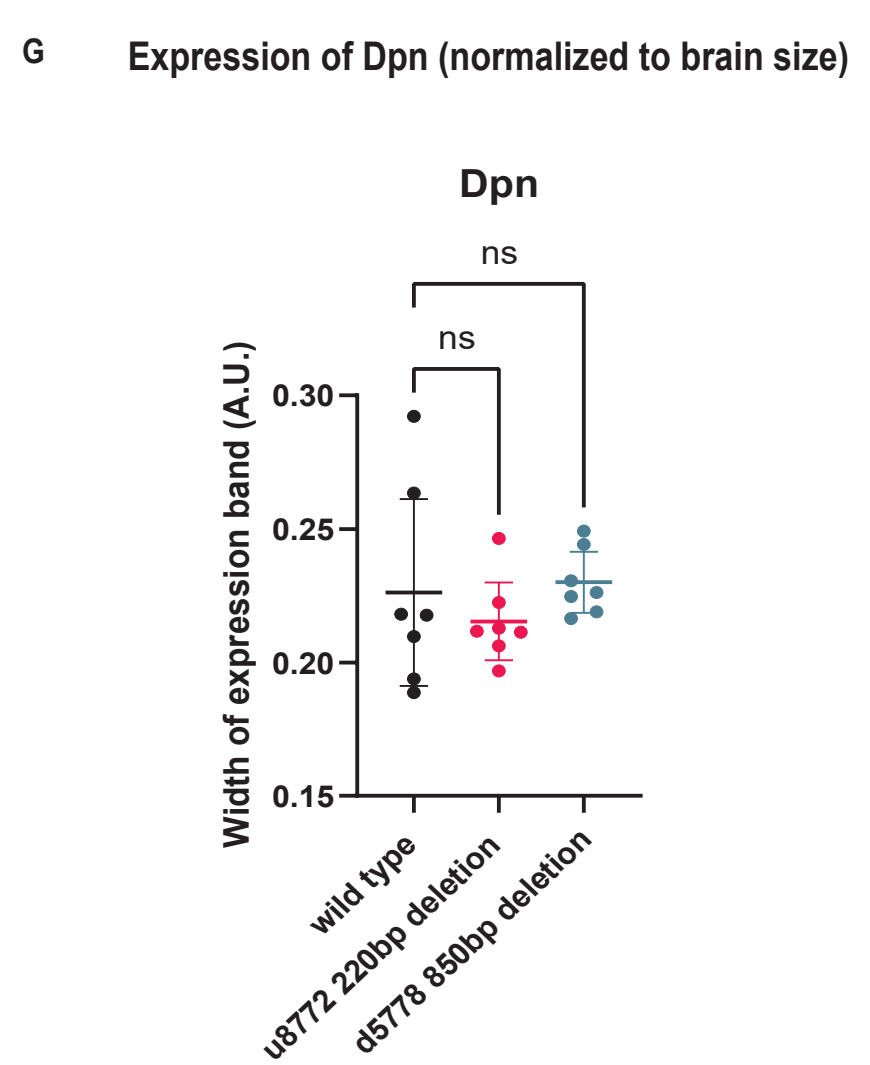

Supplementary Figure S1. Slp1/2 expression is regulated by at least two enhancers. (A-A’’’) UAS-GFP driven by GMR35H02-Gal4 is initiated at the same time as endogenous Slp1 in neuroblasts marked by Dpn. This is showing a cross-section view. (B-B’) UAS-GFP driven by GMR35H02-Gal4 perfectly overlaps with Slp2 expression. (C-D’’’) CRISPR-Cas9 deletions of the u8772 enhancer (C-C’’’) and the d5778 enhancer (D-D’’’) individually do not abolish Slp1/2 expression suggesting possible redundance. Scale bars: 20 microns. (E) Comparison of widths of expression domains normalized to brain size for Slp1 in wild type and enhancer deleted brains. P value of ordinary one way ANOVA is < 0.0001 and is statistically significant because p <0.05. Adjusted p values from Dunnett’s multiple comparison test between wild type and the u8772 220bp enhancer deletion is 0.0041, between wild type and d5778 850bp enhancer deletion is 0.0187. Both are statistically significant since p<0.05. Data from seven brains of each genotype is quantified (n=7). (F) Expression domain width normalized to brain size for Slp2 compared between wild type and enhancer deleted brains shows no statistically significant differences relative to wild type (p value from ordinary one way ANOVA =0.0019, statistically significant because p<0.05. Adjusted p values from Dunnett’s multiple comparison test relative to wild type are as follows: for u8772 220bp enhancer deletion p=0.0730, for d5778 850bp enhancer deletion p= 0.0965. Neither are statistically significant since p>0.05). Data from seven brains of each genotype is quantified (n=7). (G) Expression domain width normalized to brain size for Dpn also shows no significant differences between wild type and enhancer deletion mutants (p value from ordinary one-way ANOVA is 0.5277 and is >0.05, hence not statistically significant. Adjusted p values from Dunnett’s multiple comparisons test between enhancer deletion mutants and the wild type are as follows: for the u8772 220bp enhancer deletion p=0.6310, for the d5778 850bp enhancer deletion p=0.9414. Neither are statistically significant being >0.05.) Data from seven brains of each genotype is quantified (n=7). This shows that deletion of the enhancers doesn’t affect Dpn expression.

Supplementary Figure S2

A

B

C

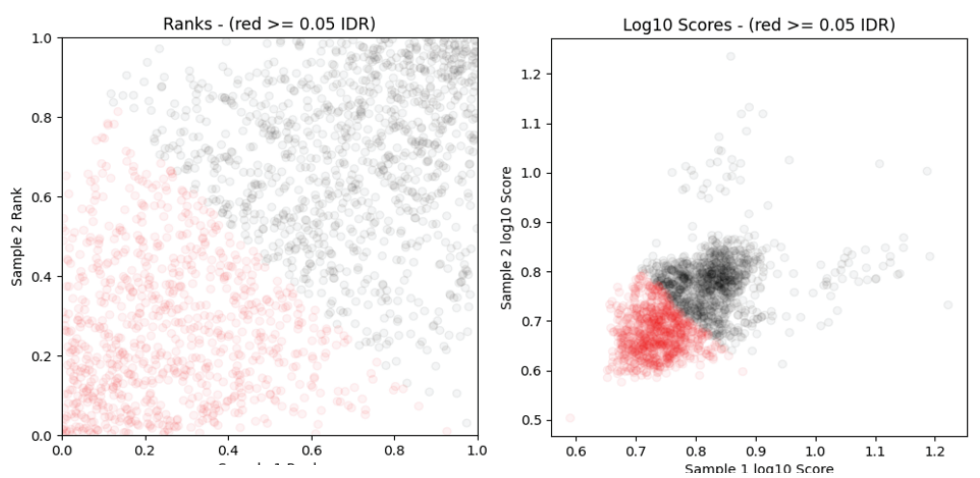

D

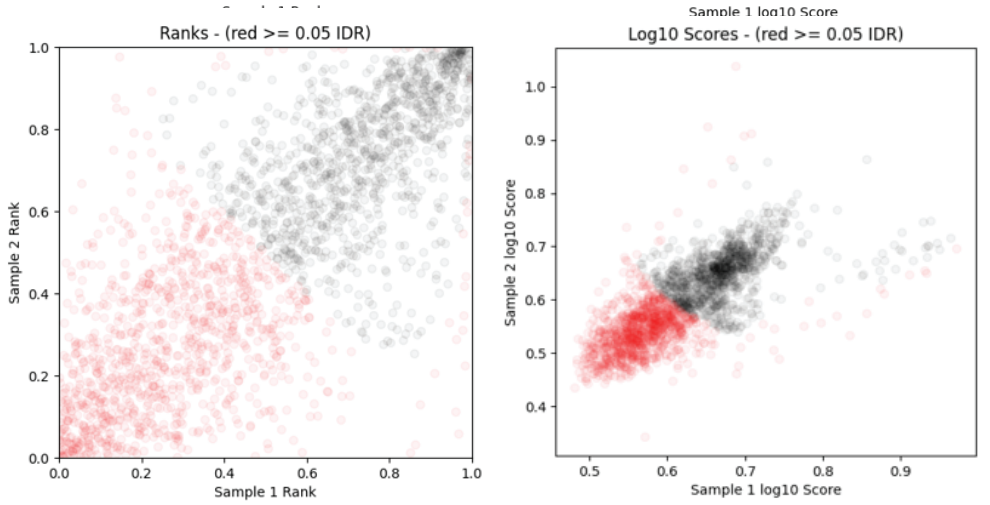

E

Transcription Factor	Number of peaks	Number of peaks passing IDR <0.05	% of peaks passing IDR <0.05
Ey-Dam	1810	984	54.4%
Su(H)-Dam	1996	972	48.7 %

Supplementary Figure S2. DamID-sequencing reveals Ey and Su(H) binding to other TTF genes. (A,B) DamID-seq also confirms EyDam and Su(H)Dam binding to *scro* (A) and *hbn* (B) loci that have been suggested by other studies to function as TTFs in optic lobe medulla neuroblasts. (C,D) Scatter plots from I.D.R. analysis of Ey-Dam (C) and Su(H)-Dam peaks (D) show reproducible peaks. Peaks represented by black dots are better reproducible and pass the I.D.R <0.05 threshold. (E) Summarized table of results from IDR analysis of Ey-Dam and Su(H)-Dam.

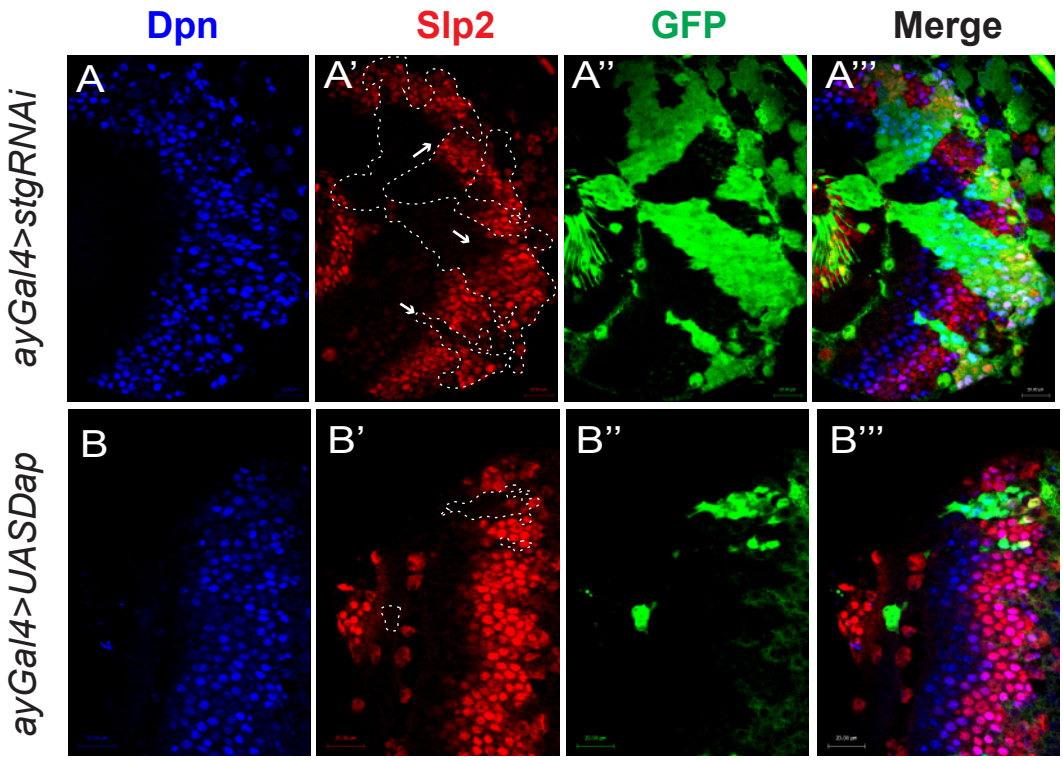

Supplementary Figure S3. Cell cycle progression is required for the temporal cascade progression. (A-A''') Larvae of genotype ywhsFLP; ayGal4UASGFP /+; UASDCR2/UASstgRNAi (VDRC 17760) were heat shocked at 37C for 8min 70 hours before dissection at 3rd instar larval stage. Dpn expression (blue) is normal in clones marked by GFP (green), while Slp2 (red) expression is delayed (11 clones). (B-B''') Larvae of genotype ywhsFLP; ayGal4UASGFP /+; UASDCR2/UAS-Dap (BDSC 83338) were heat shocked at 37C for 8min 70 hours before dissection at 3rd instar larval stage. Dpn expression (blue) is normal in clones marked by GFP (green), while Slp2 (red) expression is delayed (8 clones).